DEPARTMENT OF SCIENTIFIC AND INDUSTRIAL RESEARCH

AND

FIRE OFFICES' COMMITTEE

JOINT FIRE RESEARCH ORGANIZATION

FIRE RESEARCH NOTE

NO. 572

THE EFFECT OF WIND ON PLUMES FROM A LINE HEAT SOURCE

by

P. H. THOMAS

November, 1964.

Fire Research Station.
Boreham Wood.
Herts.
('phone ELStree 1341)

F.R. Note No. 572

DEPARTMENT OF SCIENTIFIC AND INDUSTRIAL RESEARCH AND FIRE OFFICES' COMMITTEE
JOINT FIRE RESEARCH ORGANIZATION

THE EFFECT OF WIND ON PLUMES FROM A LINE HEAT SOURCE

by

P. H. Thomas

SUMMARY

The prediction of the temperature rise downwind from a long fire front advancing in the open is of interest in the study of fire spread. This report which extends and revises an earlier report Fire Research Note 510 presents a simplified correlation in terms of dimensionless variables of the experimental data published by Rankine on the effect on the downwind temperature rise of the heat output from a line burner and the wind speed. Despite some variations of temperature rise with the absolute values of the wind speed and heat output other than those accounted for by the dimensionless variables, the correlations are on the whole satisfactory.

Applying the experimental results to a simplified theoretical model first discussed by G. I. Taylor assuming a uniform wind velocity U_o and allowing only for vertical diffusion with a diffusivity increasing in proportion to x the distance from the burner, or to the local height of the plume, gives a diffusivity ϵ_T equal to $\frac{0.048\, x\, U_o}{\Omega^{1.95}}$

where Ω is the ratio of U_o to the velocity $v = \left(\frac{gQ}{\rho c T_o}\right)^{\frac{1}{3}}$

g is the acceleration due to gravity

Q is the rate of heat release per unit length of fire

ρ is the density of air

c is the specific heat of air

and T_o is the absolute temperature

The simplified theory employed was shown by G. I. Taylor to be not entirely self consistant and this is discussed further.

The most immediately practically useful result is that over the range of dimensionless wind speeds in these experiments the maximum temperature rise at a distance x downwind is near the ground and given by

$$\theta = 2.35\, \frac{v^2\, T_o}{g x}\, \Omega^{0.14}$$

or roughly

$$\theta = 2.5\, \frac{v^2\, T_o}{g x}$$

THE EFFECT OF WIND ON PLUMES FROM A LINE HEAT SOURCE

by

P. H. Thomas

Introduction

During the last war the possibility was examined of clearing airfields of fog by using line sources of heat to set up a horizontal flow of air near the ground[1] and as part of the investigation Rankine[2] studied the effect of wind on the flow from a long line burner in the Empress Hall, Earls Court, London. Air was drawn by a large fan across a long line burner and extensive velocity and temperature measurements were made. In addition some full scale tests were undertaken in the open and satisfactory agreement was obtained between the field and laboratory experiments. Such experiments are of considerable interest in the study of the effect of wind on the spread of a long fire front and in this paper the experimental results tabulated by Rankine are correlated by dimensionless variables. At long distances from a finite source the diffusion of the plume is controlled by the turbulence in the wind and the role of thermal instability is negligible. The upper edge of the plume would appear to diverge from a source above the ground by an amount dependant on the buoyancy. Near to the real source the effects of buoyancy are predominant and these results are examined on this basis. Some observations are made regarding these various assumptions and other aspects of the problem which have been studied theoretically by Sir Geoffrey Taylor [3][4].

Results obtained by Rankine

Fig 1 shows diagrammatically the experimental arrangement and also defines the measured quantities. The ranges of the independent variables and the positions at which the temperature rise and velocity were measured are given in Table 1.

TABLE 1

The Range of Experimental Variables

Gross heat output per unit length of burner	Wind speed U_o	Distances downwind x	Heights above ground z
0.04 - 0.48 Therms per hour per yard in steps of 0.04 1 Therm = 100,000 Btu	$1\frac{1}{2}$ - 5 ft/s in steps of $\frac{1}{2}$ ft/s	3' 9", 7' 6" and 15'	1.6" to 80"

Rankine states that "the results have been analysed, interpolated and smoothed to remove evident errors in the customary manner". He did not in his tabulation of the data include any temperature rises over 30°C, and he estimated from a heat balance the net convection flux to be 80 per cent of the gross input. Of the remaining 20 per cent the major portion (15 per cent of the total) was lost as thermal radiation, presumably largely from the flames. The remaining 5 per cent was taken to be lost to the ground. This constant factor of 80 per cent is used throughout this paper to convert the tabulated gross values to net values of convected heat. The results are given in Rankine's report in tables for each value of distance x downwind from the line burner and the height z above the ground, each table giving either the temperature or horizontal velocity for all heat flows and wind speed U_o.

Scaling Laws

Let Q be the net convective flux per unit length of line per unit time, (i.e. 0.8 of the tabulated value), U the local horizontal velocity, U_o the applied wind (free stream velocity) T_o the absolute ambient temperature, ρ the density of air, c the specific heat of air, g the gravitational acceleration, and θ the rise in temperature at a distance x downwind from the line burner, and a height z above the ground.

The following assumptions are made here.

1. The effects of changes in density other than those on the buoyancy are negligible i.e. $\theta \ll T_o$.

2. The gases obey the ideal gas laws so that the effect of buoyancy is a force per unit mass of $g\,\theta/T_o$.

3. The main effect of friction with the ground is confined to a thin layer near the ground. Outside this layer mixing is assumed to be controlled primarily by turbulence generated by thermal instability, an assumption which is discussed further in the Appendix.

4. The flow outside this ground layer is assumed to be independent of viscous forces.

Either from the differential equations governing the heat balance and the momentum, or from a direct dimensional analysis of the above terms it follows that the solution takes the form

$$\phi = \frac{g\,\theta\,x}{T_o\,v^2} = F\left(\Omega, \frac{z}{x}\right) \qquad (1)$$

where Ω is the dimensionless wind speed $\frac{U_o}{v}$

and $v = \left(\frac{g\,Q}{\rho c T_o}\right)^{\frac{1}{3}}$

ϕ may be regarded as a dimensionless temperature rise.

Equation (1) is more general than Rankine's own statement regarding scaling which is physically equivalent. The data tabulated by Rankine have been used to obtain both ϕ and U/U_o as functions of z/x for different values of Ω and alternatively, as functions of Ω for different values of z/x.

Variation in temperature

Rankine's data have been evaluated in terms of the dimensionless ϕ and Ω with $\rho = 0.08$ lb/ft^3, $c = 0.24$ Btu lb^{-1}°F^{-1} $T_o = 500$°R. The accuracy of the temperature measurement was reported to be about 0.2°F and only one decimal place was given in the averages recorded. Temperature rises equal to or less than 0.3°F have therefore been omitted from the dimensionless temperature rises shown in Fig. (2 - 14). It is seen that except near the cold upper edge of the plume (Fig. 2, 3 and 4) where any experimental error is of most consequence, and near the ground (Fig. 9-14) the different sets of data are reasonably well correlated together; e.g. the one graph of Fig. (5) includes all the data in three of Rankine's tables. For the results in Fig. (7) there is a slight tendency for absolutely higher windspeeds to give absolutely higher temperatures than expected on the basis of the preceding argument and the effect is more pronounced at 15' than at 7' 6" from the burner. At the higher speeds the results for the two different positions are in closer agreement than at lower speeds.

In Fig. (9-14), which pertain to a region close to the ground $\left(\frac{z}{x} \ll 0.11\right)$

where the flow was thermally stratified there is a general tendency at high wind speeds for an increase in the speed to increase the temperature at the measuring point. There is a noticeable variation in ϕ with the absolute wind speed as well as with the dimensionless wind speed Ω, and for each velocity, ϕ usually has a minimum Fig. (9, 11, 12 and 14) which occurs at a value of Ω approximately proportional to U_o i.e. at the same value of ν for each.* However the effect is absent or ill-defined at 7' 6" the middle (see Fig. 10 and 13) of the three distances downwind at which measurements were made. This apparent lack of systematic behaviour means further study is necessary before conditions near the ground in these experiments could be discussed in much further detail.

Except near the ground the lack of correlation, although systematic as in Fig. (7), is slight. If from Fig. (2-14) we take a series of values of ϕ throughout the range of Ω and from the smoothed curves plot ϕ against z/x we obtain the curves in Fig. (15). For Fig. (10) and (13) the upper line was used. Obviously the part of the profile near the ground is not expected to be accurate. It will be noticed in Fig. (15) that above z/x equal to about 0.1 increasing the wind reduces the temperature; below z/x about 0.1 it increased it.

The variation in local velocity

In the velocity profiles given by Rankine for the unheated condition the velocity U was found to be proportional to U_o and independent of x. U/U_o is plotted against $\log_e z$ in Fig. (16). From the profile equation

$$U = 2.5\, U^x \log_e z/z_o$$

the friction velocity U^x is obtained as

$$U^x = 0.047\ U_o$$

and the characteristic roughness z_o as

$$z_o = 0.029 \text{ cm} = 0.00075 \text{ ft}$$

The macro-viscosity $U^x z_o$ varied from 53×10^{-6} ft^2/s to 170×10^{-6} ft^2/s so that flow was intermediate between smooth and fully rough. Z_o is sufficiently large for it to be effectively independent of U_o. The skin friction coefficient C_f taken as $2\left(\frac{U^x}{U_o}\right)^2$ is equal to 0.0045. The eddy viscosity near the wall is $0.4\, U^x z$

$$\text{i.e. } \epsilon_v = 0.019\, U_o z \qquad (3)$$

and this would obtain for zU^x/ν below about 100. With ν the kinematic viscosity 150×10^{-6} ft^2/s, and U_o in these experiments in the range $1\frac{1}{2}$ ft/s to 5 ft/s it follows that equation (3) applies for z less than about 3". In this region, no velocity measurements were made and the temperature rises were measured only at z = 1.6" at 3' 9", 7' 6" and 15' from the burner.

At values of $z\,U^x$ greater than about 100 the eddy viscosity, according to Clauser (5) has a uniform value

$$\epsilon_v = 0.018\ U_o \delta^* \qquad (4)$$

where δ^* is the displacement thickness and

$$\delta^* = \int_o^\infty (1 - U/U_o)\, dz$$

A graphical integration of the profile where there was no heating gave

$$\delta^* = 0.43 \text{ ft.}$$

---

*This was drawn to my attention by Dr. B. R. Morton

so that for these experiments ϵ_v reached a maximum value varying from 0.012 ft^2/s to 0.04 ft^2/s over the range of wind speed. It is shown in the Appendix that in the range of these experiments this is at most $\frac{1}{3}$ of the eddy viscosity calculated from thermal instability and in the middle of the experimental range an order less. When Q was not zero and the wind speed not too high the velocity profile had a maximum exceeding the main stream wind speed - see Fig. (17). Figs. (18) (19) and (20) give values of U/U_0 against Λ for various positions in the stream, each group corresponding to a particular height of the measuring point, and it can be seen that the velocity enhancement, as Rankine described it, disappears for $\Lambda > 3$ even when U_0 is as low as $1\frac{1}{2}$ ft/s. The curves of U/U_0 versus Λ show that at high values of U_0 the value of U/U_0 does not rise progressively as Λ falls. This is particularly noticeable near the ground - see Fig. (20). The value of Λ at which U/U_0 reaches a maximum is approximately proportional to U_0 i.e. the maximum U occurs at a particular value of v ($\sim$1.5 ft/s) which is close to the value which was pointed out above as marking minima in the temperature curves near the ground. At higher values of v the temperature is above and the velocity below that expected from the trend of the correlation for lower values of v.

The velocities at any one position appear to be asymptotic to a single curve for low values of U_0. There is, however, one position (Fig. 18A) where the correlation is particularly poor.

At high values of Λ the values of U tend to those typical of zero Q, where U is determined by ground friction and U/U_0 is a function of z. For non-zero Q local velocities cannot, however, be correlated in terms of Λ and $\bar{z}$. Only two comparisons are possible for equal values of z/x and different x and these (Figs. (18A) and (18B) are inconclusive.

In a vertical plume diffusion in the horizontal direction is greater than in vertical direction. For a bent over plume the reverse is true so there must be a region of low Λ where diffusion in one direction cannot be neglected in comparison with the other (i.e. no boundary layer approximation is possible) but largely because of experimental difficulties with recirculation under the roof the transition from a vertical to a horizontal plane could not be examined by Rankine.

In still air a horizontal flow is induced into a vertical plume[6] equal to $0.29v$ from each side. If the transition were a gradual one it might be expected that as U_0 decreases the horizontal velocity U should approach a limit

$$U \to 0.29v$$

$$\text{i.e.} \quad U/U_0 \to 0.29/\Lambda \quad \text{as} \quad \Lambda \to 0$$

At high values of Λ, U/U_0 might be expected to approach the limit given by the profile in Fig. (16) for zero Q, i.e. $\Lambda U/U_0$ should tend to be linear with Λ. Accordingly $\Lambda U/U_0$ has been evaluated and plotted against Λ (not shown here), but in view of the lack of correlation between data for different values of U_0 and the limited range of Λ for which there is a large enough excess of U/U_0 above its minimum value, the extrapolation to zero Λ is rather imprecise. It was possible to use six sets of data and the extrapolation gave values between 0.6 and 1.2 with a mean of 0.85. This is three times larger than the figure 0.29 and it suggests that it may not be possible to regard the limiting form of these plumes as one half of a vertical plume nor perhaps even as one half of a vertical plume entraining as much air on one side as a vertical plume entrains on both sides.

Discussion

Sir Geoffrey Taylor[3][4] considered the theoretical interpretation of this problem by assuming as an approximation that the velocity was uniform and in one direction. Only transport of heat in the z direction was allowed for. The heat balance equation then becomes

$$\rho c U_o \frac{\partial \theta}{\partial x} = \frac{\partial}{\partial z}\left(K \frac{\partial \theta}{\partial z}\right) \tag{5}$$

Two forms for the effective diffusivity were considered viz:

$$\epsilon_T = \frac{K}{\rho c} C_1 \ell \sqrt{\frac{g \theta}{T_o}} \tag{6A}$$

and

$$\epsilon_T = \frac{K}{\rho c} C_2 \ell^2 \sqrt{\frac{g}{T_o}\left|\frac{\partial \theta}{\partial z}\right|} \tag{6B}$$

where C_1 and C_2 are constants to be determined from the experiments, l is a mixing length assumed proportional to the height of the plume.

$$\ell \propto x \ \mathrm{Tan}\alpha \tag{7}$$

The constant of proportionality can be absorbed into C_1 or C_2 and α is the angle the upper edge of the plume makes with the horizontal. He assumed that there was a similarity solution such that the distribution of temperature across any vertical section of the plume was the same though the scale both of the temperature distribution and the height of the plume were assumed functions of the wind speed and the heat output. The only independent parameter in this formulation that can determine these scales is the dimensionless wind speed and he assumed a similarity solution and that the dependence of the scales on this term took the form of a power law. Equation (1) then takes the form

$$\phi = \Lambda^m G\left(\frac{z}{x \mathrm{Tan}\alpha}\right) \tag{8}$$

where

$$\mathrm{Tan}\alpha \propto \Lambda^n \tag{9}$$

The indices m and n have yet to be determined. If equations (8) and (9) are substituted into equations (5) and (6) we obtain whichever form is used for ϵ_T

$$\mathrm{Tan}\alpha \propto \Lambda^{m-2} \tag{10}$$

The heat balance is

$$\rho c \int_0^{x \mathrm{Tan}\alpha} U_o \theta_o \, dz = Q \tag{11}$$

and using equations (8) and (9) this gives

$$m + n + 1 = 0 \tag{12}$$

Equating the indices of Λ in equations (9) and (10) then gives

$$m = \tfrac{1}{2} \quad \text{and} \quad n = 3/2$$

The tangent of the plume angle should therefore vary as $Q^{\frac{1}{2}}/U^{3/2}$ and the maximum dimensionless temperature ϕ_o as $\Lambda^{\frac{1}{2}}$. These results have recently been discussed again by Sir Geoffrey Taylor[4] and he emphasized that they are a consequence of assuming that the turbulence is produced by thermal instability. If the turbulence were assumed to originate from horizontal shear then Tan α would be independent of the dimensionless windspeed. In fact the experimental

observations[2] showed that

$$\text{Tan}\alpha \propto \left(\frac{Q}{U^3}\right)^{0.286}$$

and he commented that this is intermediate between the two results and suggested that shear and thermal instability were of comparable importance. Rankine refers to field measurements 75 yds downwind and this represents a scale factor of from 15 : 1 to 60 : 1 compared with the measurements at 15' and 3' 9" in the laboratory. To obtain similarity between the effects of shear and thermal instability would require equal values of

$$\frac{U^x}{\nu} \quad \text{i.e. equal values of} \quad \sqrt{C_f}\,\mathcal{R}$$

The comparison was made at equal values of $\mathcal{R}$ so it must be deduced that the values of C_f were effectively the same or of little consequence.

However there is an interesting alternative. Equations (6a) and (6b) are both based on the view that the characteristic mixing length is proportional to l the local height of the plume on the assumption that plumes (and jets) are in local equilibrium. Maczynski[7] has recently argued that this fails for a jet injected into a stream moving in the same direction and showed that his results were in accordance with the characteristic mixing length being proportional to the distance from the source.

If ϵ_T is written as

$$\epsilon_T = \frac{K}{\rho C} = C_1' x \sqrt{\frac{g\theta l}{T_0}} \qquad (13A)$$

or

$$\epsilon_T = \frac{K}{\rho C} = C_2' x \sqrt{\frac{g}{T_0}\left(\frac{\partial\theta}{\partial z}\right) l^2} \qquad (13B)$$

we obtain on substituting equations (7) (8) and (9) into equations (5) and (13)

$$\text{Tan}\,\alpha \propto \mathcal{R}^{\frac{m}{3}-\frac{2}{3}} \qquad (14)$$

Equating the indices in equation (9) and (14) and using equation (12)

we obtain $\quad m = -\frac{1}{4} \quad$ and $n = -\frac{3}{4}$

Hence Tan α is proportional to $\mathcal{R}^{-\frac{3}{4}}$ i.e. the tangent of the plume angle varies as $Q^{\frac{1}{4}}/U_0^{\frac{3}{4}}$ and this is very close to the experimental result of $\mathcal{R}^{-0.86}$ as given by Rankine. In accordance with this and the assumption of a uniform velocity we obtain

$$\phi = \mathcal{R}^{-\frac{1}{4}} \mathcal{G}\left(\frac{z}{x}\mathcal{R}^{\frac{3}{4}}\right)$$

It can readily be shown that $\phi\mathcal{R}^{\frac{1}{4}}$ and $(z/x)\mathcal{R}^{\frac{3}{4}}$ correlate the data better than do $\phi\mathcal{R}^{-\frac{1}{2}}$ and $(z/x)\mathcal{R}^{3/2}$ but in fact no pair of variables of the form $\phi\mathcal{R}^{M}$ and $(z/x)\mathcal{R}^{1-m}$ is satisfactory. For low values of $\mathcal{R}$ the value of U/U_0 is noticeably larger than 1 and there are insufficient data for $\mathcal{R} > 2$ to provide a satisfactory test of a simplified theory assuming U is constant. Fig. (21) shows an empirical correlation between $\phi\mathcal{R}^{0.14}$ and $z/x\,\mathcal{R}^{0.75}$. For many practical purposes it will be necessary only to estimate the maximum temperature rise downwind and this is seen from Fig. (21) to be approximately given by

$$\theta = 2.35\,\frac{\nu^2 T_0}{g\,x}\,\mathcal{R}^{0.14}$$

Since $\mathcal{R}^{0.14}$ varies only slightly in the range $1 < \mathcal{R} < 3$

$$\theta = 2.5\,\frac{\nu^2 T_0}{g\,x}$$

It is shown in the Appendix that it is possible from the experimental data to express ϵ_T as

$$\epsilon_T = \frac{0.048\ U_o{}^x}{\Lambda^{1.95}}$$

Equation (13) would, however, lead to ϵ_T being proportional to $\Lambda^{-1.5}$ instead of the Λ^{-3} from equation (6). The above expression for ϵ_T should give Tan α as proportional to $\Lambda^{-0.98}$ but the temperature profiles show this is a little too large a dependence on Λ. A model assuming a constant plume angle and a diffusivity proportional to either the distance from the burner or the height of the plume and a velocity having the dimensional form $\sqrt{\frac{g\theta l}{T_o}}$ i.e. either of equation (13) or the modification of it used in the Appendix is thus not entirely self consistent.

The conclusion from the arguments given above would seem to be that the values of Λ although sufficiently high to make the plume bend over are not all sufficiently high for it to be considered as a fully horizontal plume in the sense demanded by the assumption of a uniform horizontal velocity and negligible horizontal diffusion. The difficulties in accepting that the ground friction is of comparable importance to the thermal instability can be partially met if the mixing length is determined by the distance from the heat source instead of the distance from the ground.

References

(1) "The Dispersal of Fog from Airfield Runways" ed. Walker R. G. and Fox D. A. Min. of Supply. London, 1946.

(2) RANKINE, A. O. "Experimental Studies in Thermal Convection" Proc. Phys. Soc. London, 1950 63 Part 5. (365A) 417.

(3) TAYLOR, G. I. - see Appendix E of ref. (1).

(4) TAYLOR, G. I. "Fire under influence of Thermal Convection" International Symposium on the Use of Models in Fire Research (1959) p.10. Publication 786, National Academy of Science National Research Council. Washington D.C.

(5) CLAUSER, F. H. "The Turbulent Boundary Layer" Advances in Applied Mechanics, New York 1956, 4 1-51.

(6) ROUSE HUNTER, YIH, C. S. and HUMPHREYS, H. W. "Gravitational Convection from a Boundary Source". Tellus (1952) 4, 210.

(7) MACZYNSKI, J. F. J. "A round jet in an ambient co-axial stream". J. Fluid Mechanics (1962) 13 p.597.

APPENDIX

A value for the Effective Diffusivity

To obtain numerical values of ϵ_T from the data we shall assume that ϵ_T is independent of z, i.e. it is constant across the height of the plume at any section.

If as an approximation U is taken as constant equal to U_o equation (5) may be written from equation (1) as

$$\left(\frac{\epsilon_T}{U_o x}\right) \phi'' + \lambda \phi' + \phi = 0 \qquad (15i)$$

where the dash denotes differentiation with respect to λ $(= \frac{z}{x})$. ϵ_T $(= \frac{K}{\rho c})$ is proportional to the distance from the burner or the height of the plume; in either case $\frac{\epsilon_T}{U_o x}$ is independent of λ. If λ_o is the value of λ at which ϕ is zero, equation (14) becomes

$$\phi = \phi_o \, e^{-\frac{U_o x}{2\epsilon_T}(\lambda - \lambda_o)^2} \qquad (15ii)$$

where ϕ_o is the value of ϕ at λ_o. Figure (15) shows that λ_o is approximately between 0.08 and 0.10. Figure (22) shows Log ϕ plotted against $(\lambda - \lambda_o)^2$ with values of ϕ taken from the curves of ϕ against λ for various z and x and $\lambda_o = 0.09$. There are few data in the outer region of the heated flow but they suggest that the regime changes for $\phi < 0.1$, where all the data comprise temperature rises of less than 2^oF. Apart from this outer region and the stratified layer near to the ground the data lie on straight lines, the negative slope increasing with λ. This set of data are shown in a different form in Fig. (23) where no assumption is made regarding λ_o but the data are plotted in terms of an estimate of ϕ_o. Here too the lines are straight.

For simplicity we shall take the square root term in the expression for ϵ_T as $\sqrt{\frac{g}{T_o}\int_0^{x\tan\alpha} \theta\, dz}$ instead of the forms in equations (6A) and (6B). This is dimensionally of the same form and the difference will be partly absorbed by the constant of proportionality.

We now write

$$\epsilon_T = C_3 x \, (\tan\alpha)^p \sqrt{\frac{g}{T_o}\int_0^{x\tan\alpha} \theta\, dz} \qquad (16)$$

where $p = 1$ if the mixing length is proportional to the height of the plume and zero if it is proportional to the distance from the burner.

From equation (15) we have

$$\tan\alpha \propto \sqrt{\frac{\epsilon_T}{U_o x}} \qquad (17)$$

From the heat balance equation (11)

$$\int_0^{x\tan\alpha} \frac{\theta\, dz}{T_o} = \frac{Q}{\rho c T_o U_o} \qquad (18)$$

so that from equations (16) (17) and (18)

$$\left(\frac{\epsilon_T}{U_o x}\right)^{1-p/2} \propto \frac{1}{\lambda^{3/2}}$$

i.e. $$\frac{U_0 x}{\epsilon_T} \propto \Omega^{\frac{3}{2-p}}$$

The inverses of the slopes from Figs. (22) and (23) are plotted in Fig. (24) against Ω for seven chosen values of Ω in the range $1 < \Omega < 3$.

The line drawn through the points corresponds to

$$\epsilon_T = \frac{0.048\ U_0 x}{\Omega^{1.95}}$$

The dependence of ϵ_T on Ω is greater than that corresponding to p = 0 but differs from it by more from that corresponding to p = 1. The above result would imply that Tan α varies almost inversely proportionally to Ω but the correlation in Fig. (21) would be less satisfactory if this were used instead of $\Omega^{-0.75}$. The correlation of the results with this type of theory is therefore not entirely consistent. The ratio of ϵ_T to ϵ_V in equation (4) is

$$\frac{\epsilon_T}{\epsilon_V} = \frac{0.048}{0.018 \delta^* \Omega^{1.95}} \frac{x}{} = \frac{2.7}{\delta^* \Omega^{1.95}}$$

The minimum value of x/δ^* in these experiments is $\frac{3.75}{0.43} = 8.7$ and Ω is less than 3.

$$\therefore \quad \frac{\epsilon_T}{\epsilon_V} > \frac{2.7 \times 8.7}{8.6} \sim 2.7$$

In the middle of the range x is 7 ft 6 in and $\Omega = 2$ so that there $\frac{\epsilon_T}{\epsilon_V} \sim 10$. Thus except at the positions nearest the burner, at the highest wind speed and lowest heat output the effects of thermal instability are expected to be predominant.

Nearer the burner the value of ϵ_T decreases relative to ϵ_V but the effective thickness of the plume becomes less and it becomes more appropriate to use equation (3) for ϵ_V. The value of z is less than x Tan α so one can obtain the minimum value of the ratio of ϵ_T to ϵ_V as

$$\frac{\epsilon_T}{\epsilon_V} > \frac{0.048}{0.019} \frac{1}{\text{Tan}\alpha\ \Omega^{1.95}}$$

Tan α from Fig. (15) may be taken as approximately $0.7/\Omega^{\frac{3}{4}}$ so that $\frac{\epsilon_T}{\epsilon_V} > 3.4/\Omega^{1.2}$

Over the range of Ω used in the experiments this ratio varies from about 0.9 to 3.4 and so near the burner it is not possible to disregard either thermal instability or shear. Whether ϵ_T depends on the distance from the burner or on the height of the plume the implication of the above is that thermal instability becomes more important as x increases, provided the forms taken for ϵ_V still apply. This of course is not so for all x. Beyond a distance from a finite line source where the lateral diffusion of heat and the loss of heat to the ground become significantly large buoyancy per unit width of plume is no longer conserved as is implied by the use of equation (18).

Acknowledgements

The author would like to thank Messrs. Naughton and Theobald for assistance with calculating the data in dimensionless form.

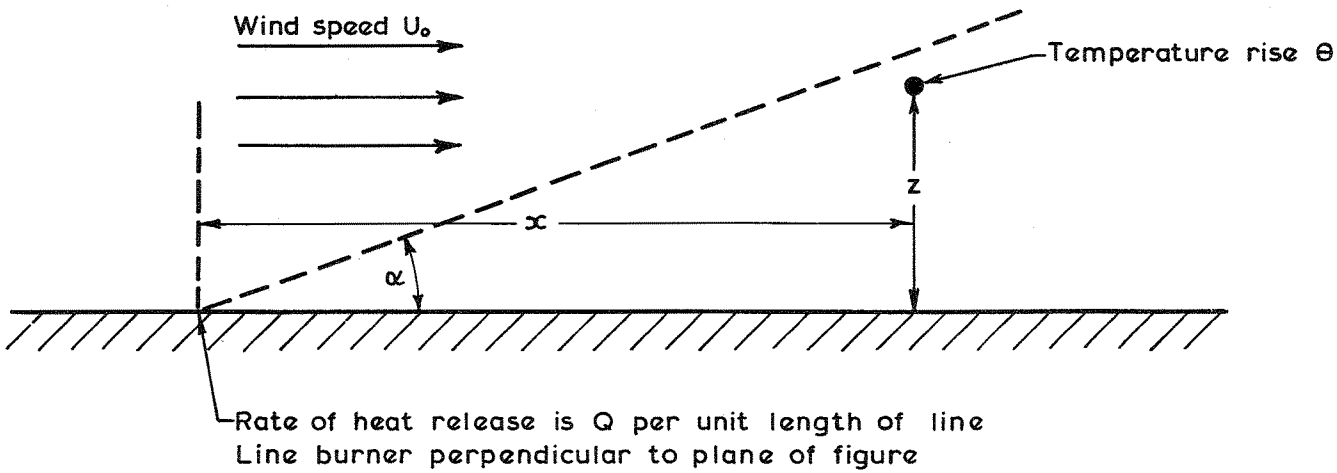

FIG. 1. DIAGRAMMATIC REPRESENTATION OF FLOW SYSTEM

1/5700 F.R. 572

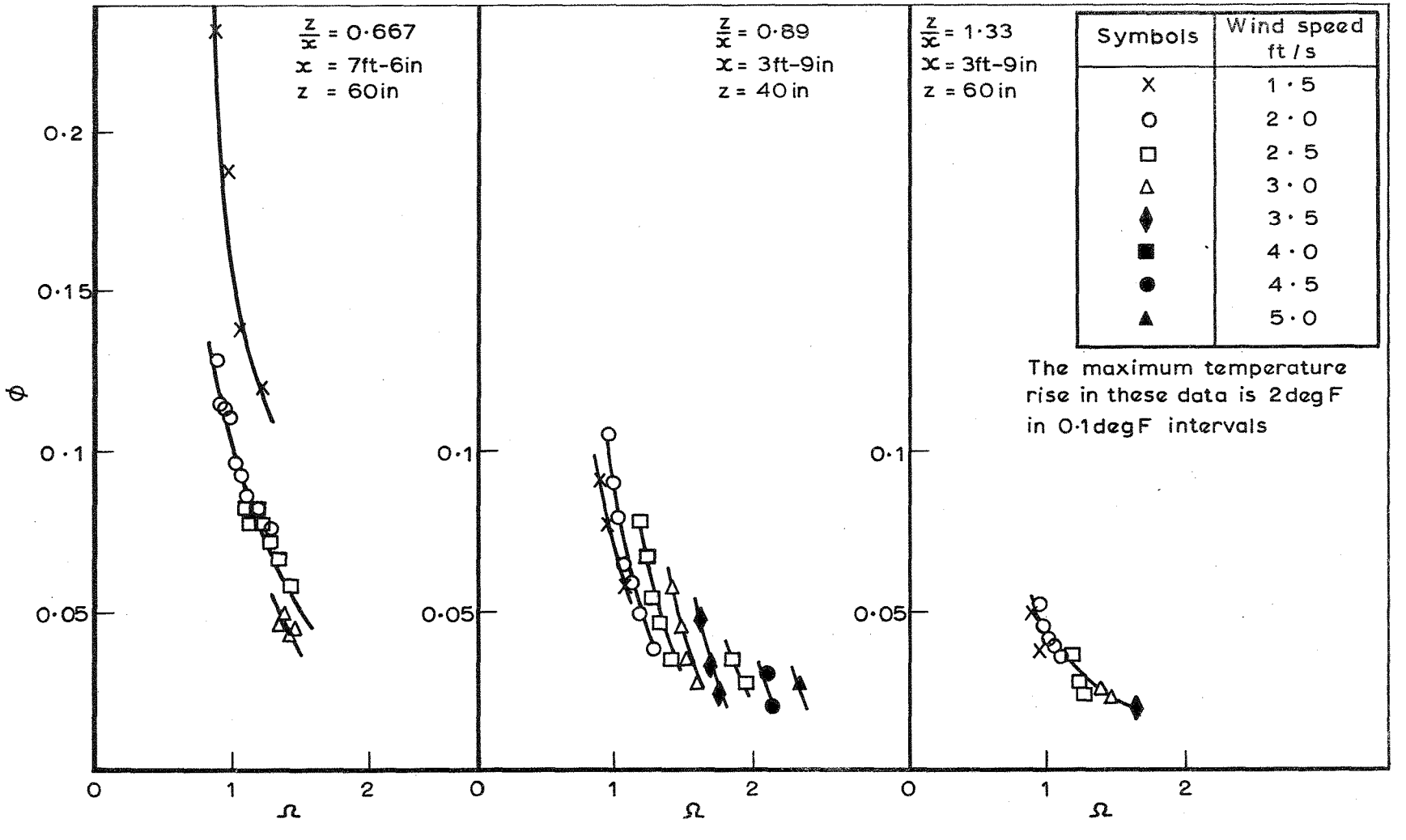

FIGS. 2, 3 AND 4. DIMENSIONLESS TEMPERATURE RISES

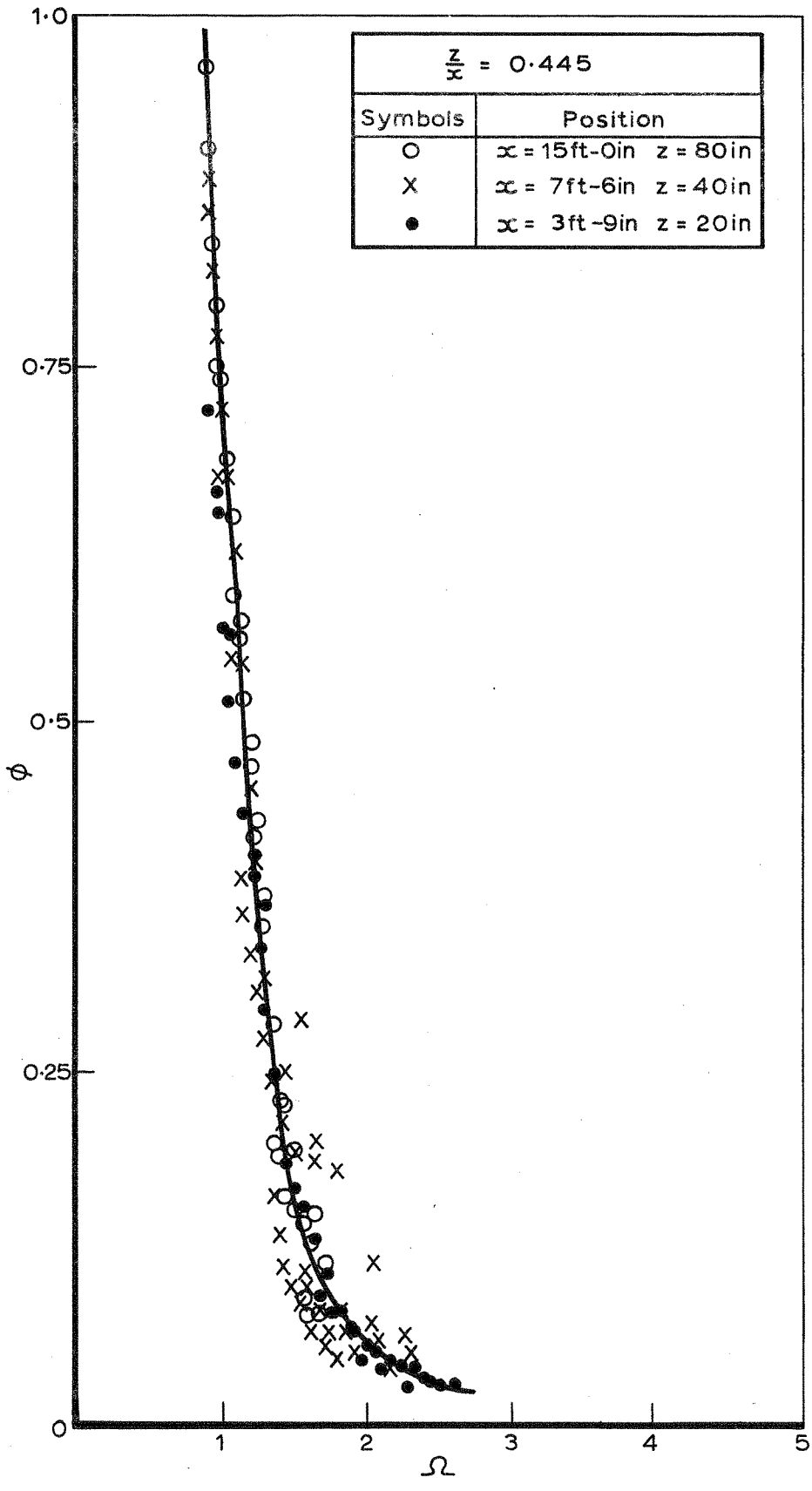

1/5701 F.R. 572

FIG. 5. DIMENSIONLESS TEMPERATURE RISES

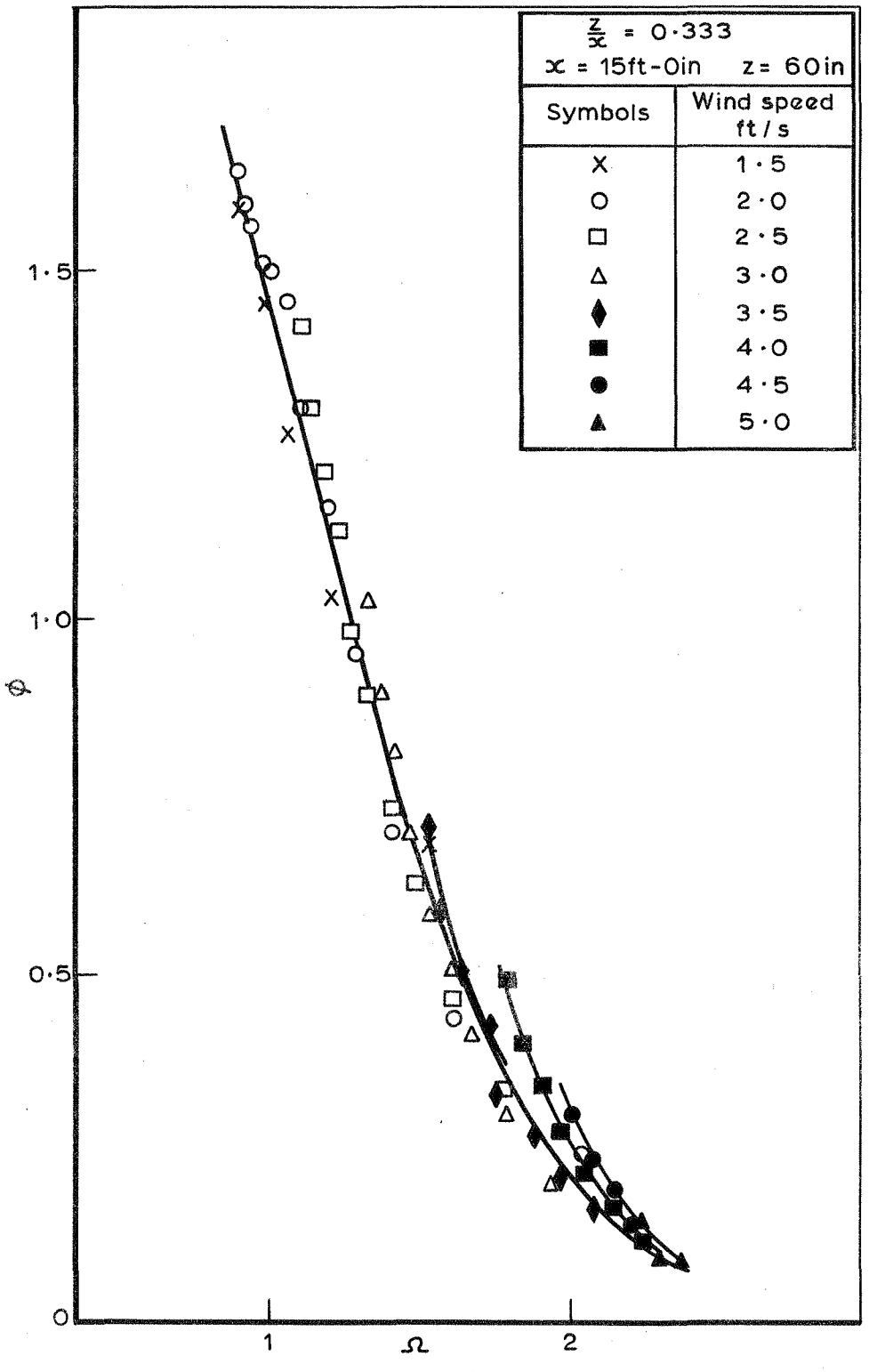

FIG. 6. DIMENSIONLESS TEMPERATURE RISES

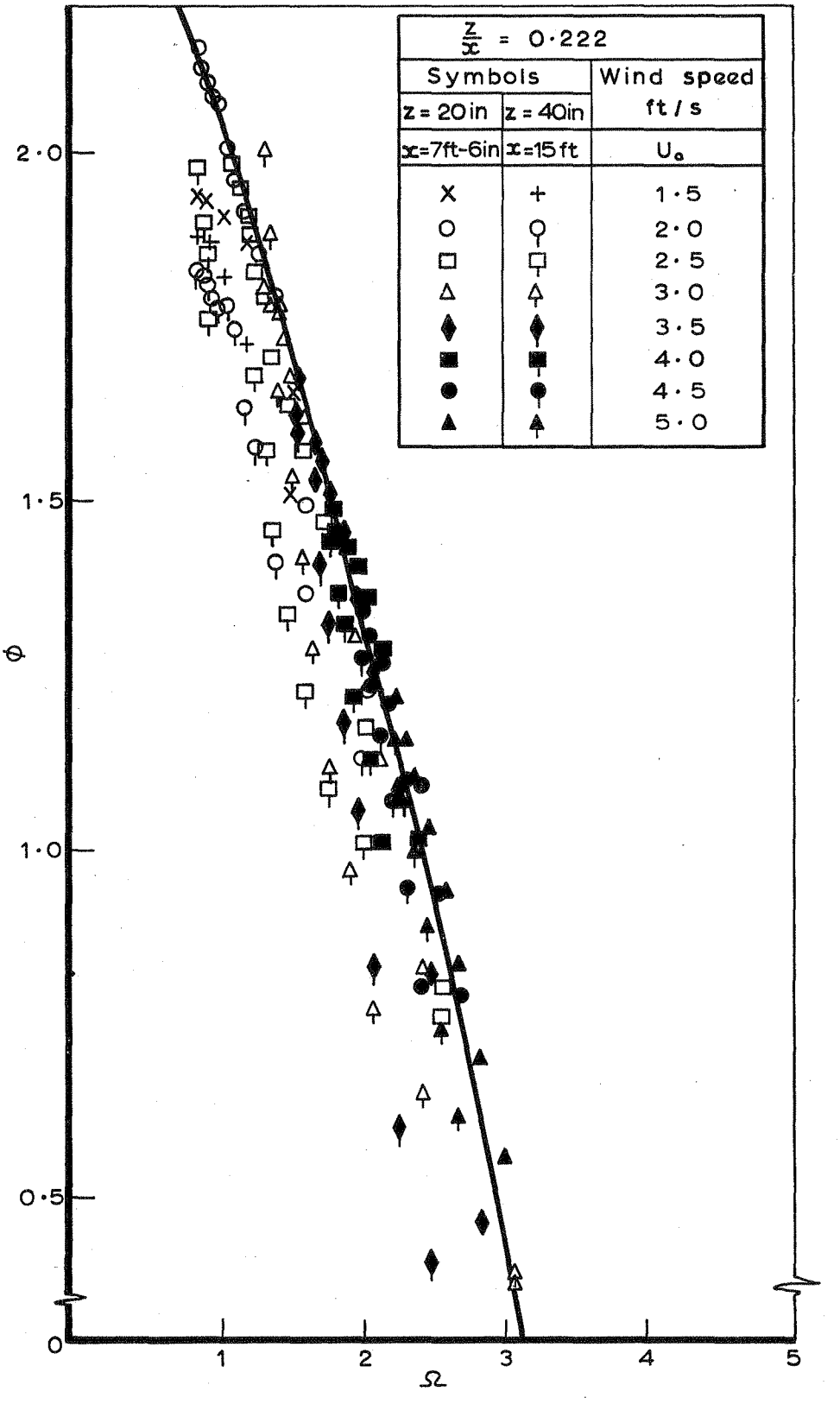

1/5703 F.R. 572

FIG. 7. DIMENSIONLESS TEMPERATURE RISES

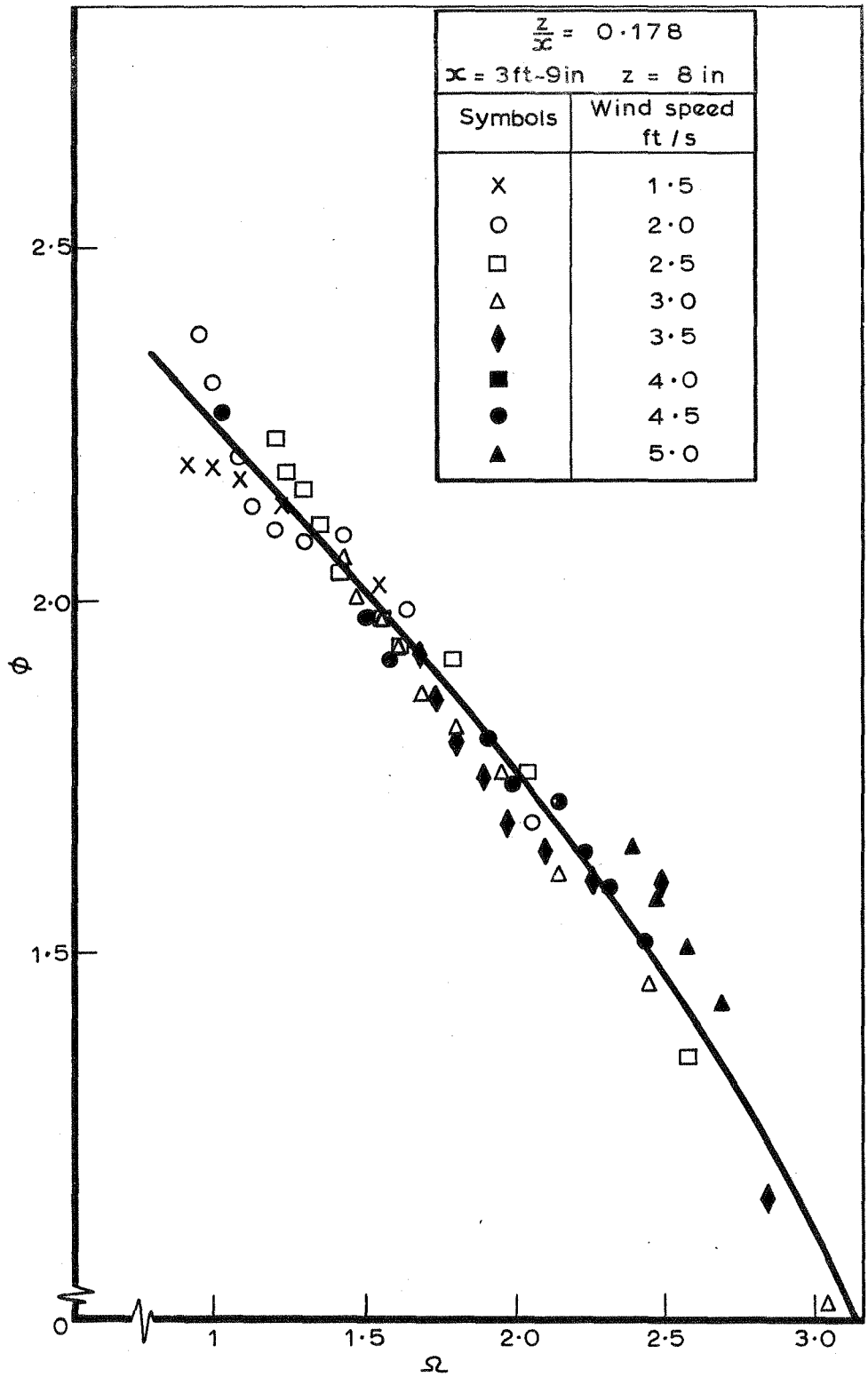

FIG. 8. DIMENSIONLESS TEMPERATURE RISES

1/5704 F.R. 572

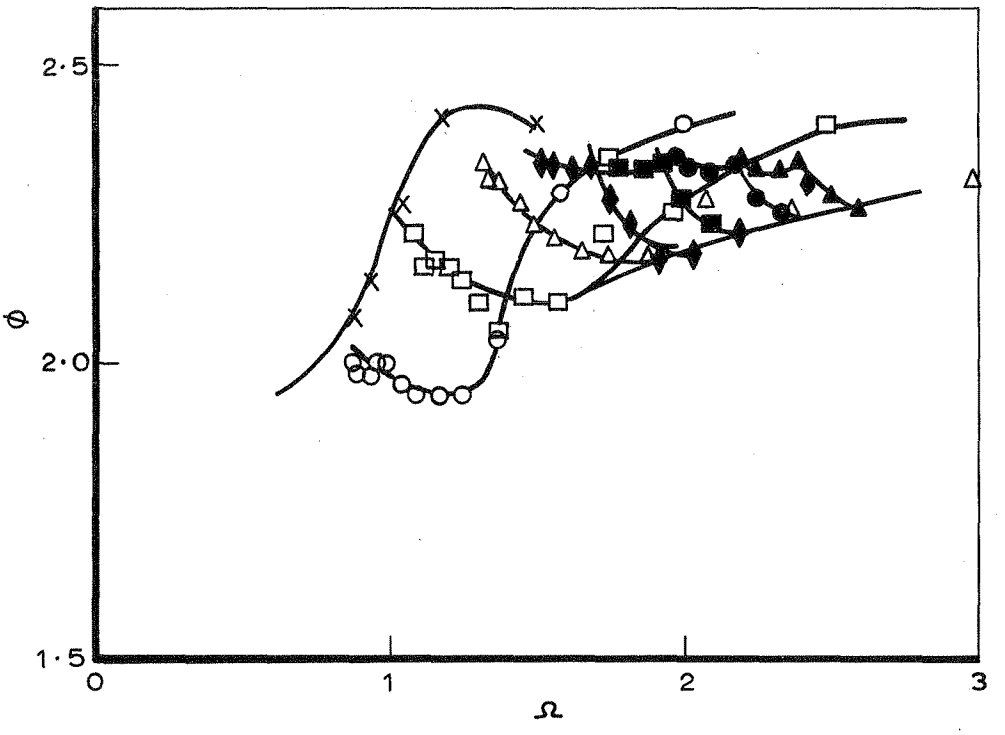

$\frac{z}{x} = 0{\cdot}111$	
x = 15ft–0in	z = 20 in
Symbols	Wind speed ft/s
X	1·5
O	2·0
□	2·5
△	3·0
♦	3·5
■	4·0
●	4·5
▲	5·0

FIG. 9. DIMENSIONLESS TEMPERATURE RISES

1/5705 F.R. 572

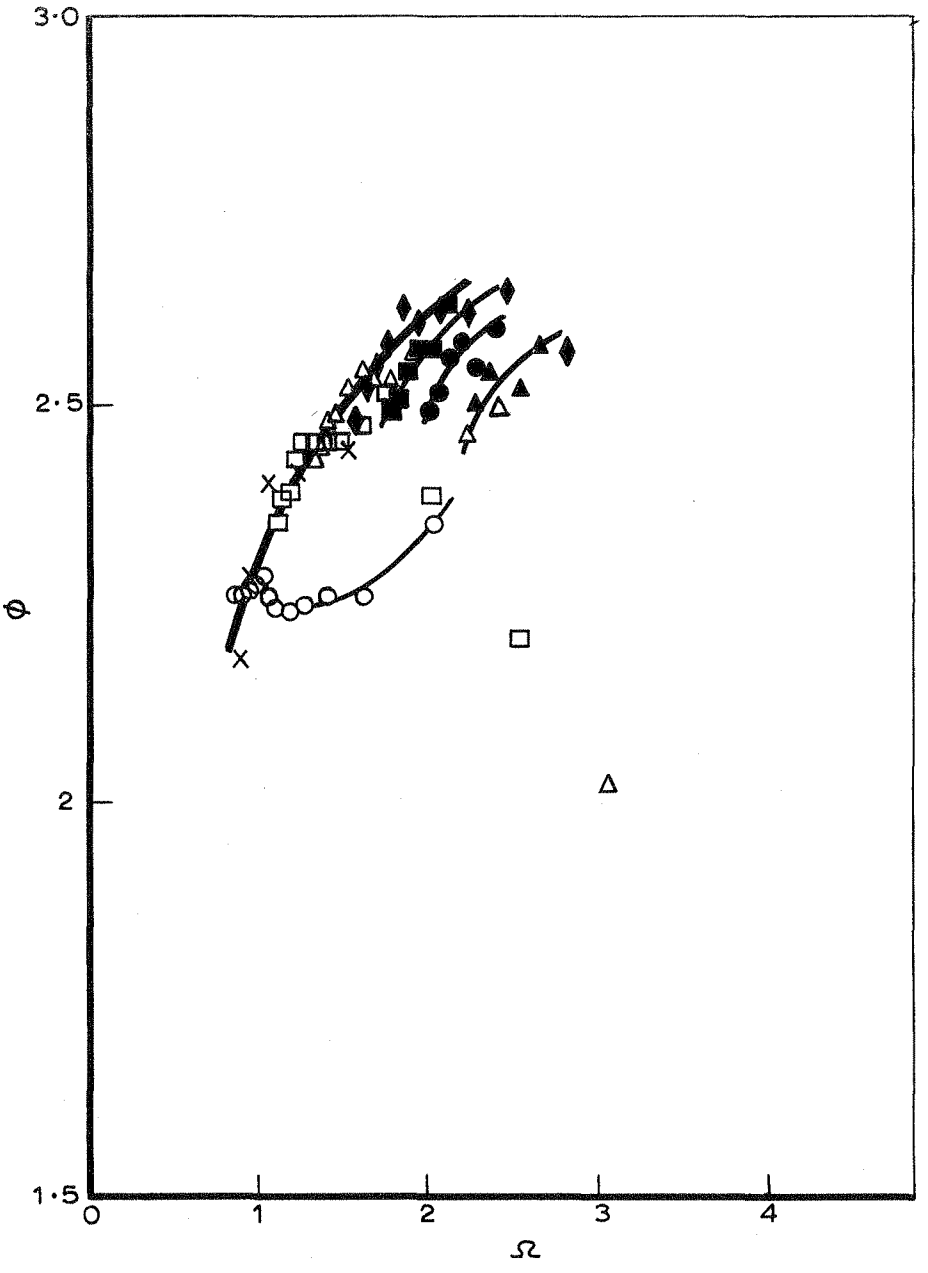

$\frac{z}{x}$ = 0·089 x = 7ft-6in z = 8in	
Symbols	Wind speed ft/s
X	1·5
O	2·0
□	2·5
Δ	3·0
♦	3·5
■	4·0
●	4·5
▲	5·0

1/5706 F.R. 572

FIG. 10. DIMENSIONLESS TEMPERATURE RISES

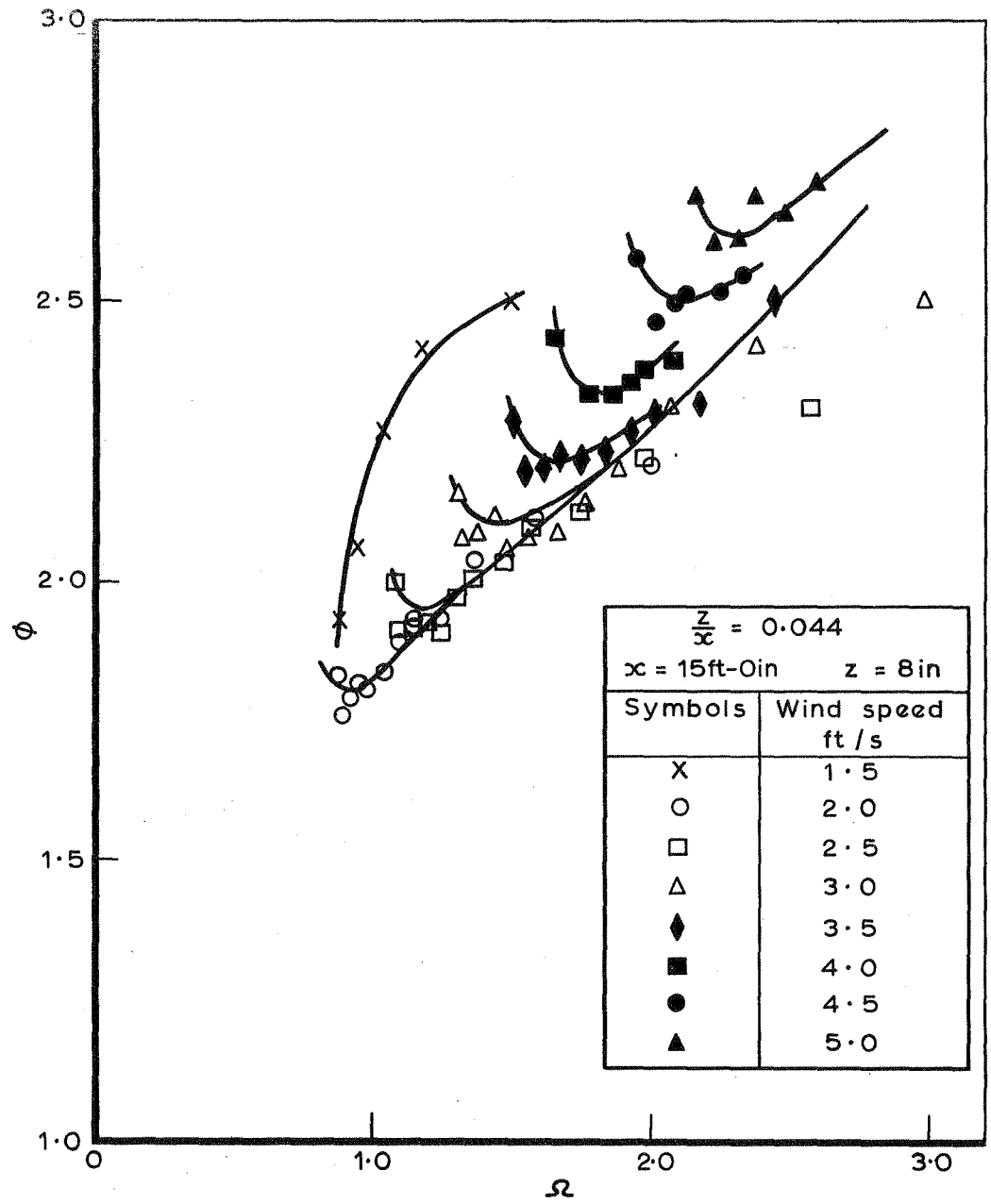

FIG. 11. DIMENSIONLESS TEMPERATURE RISES

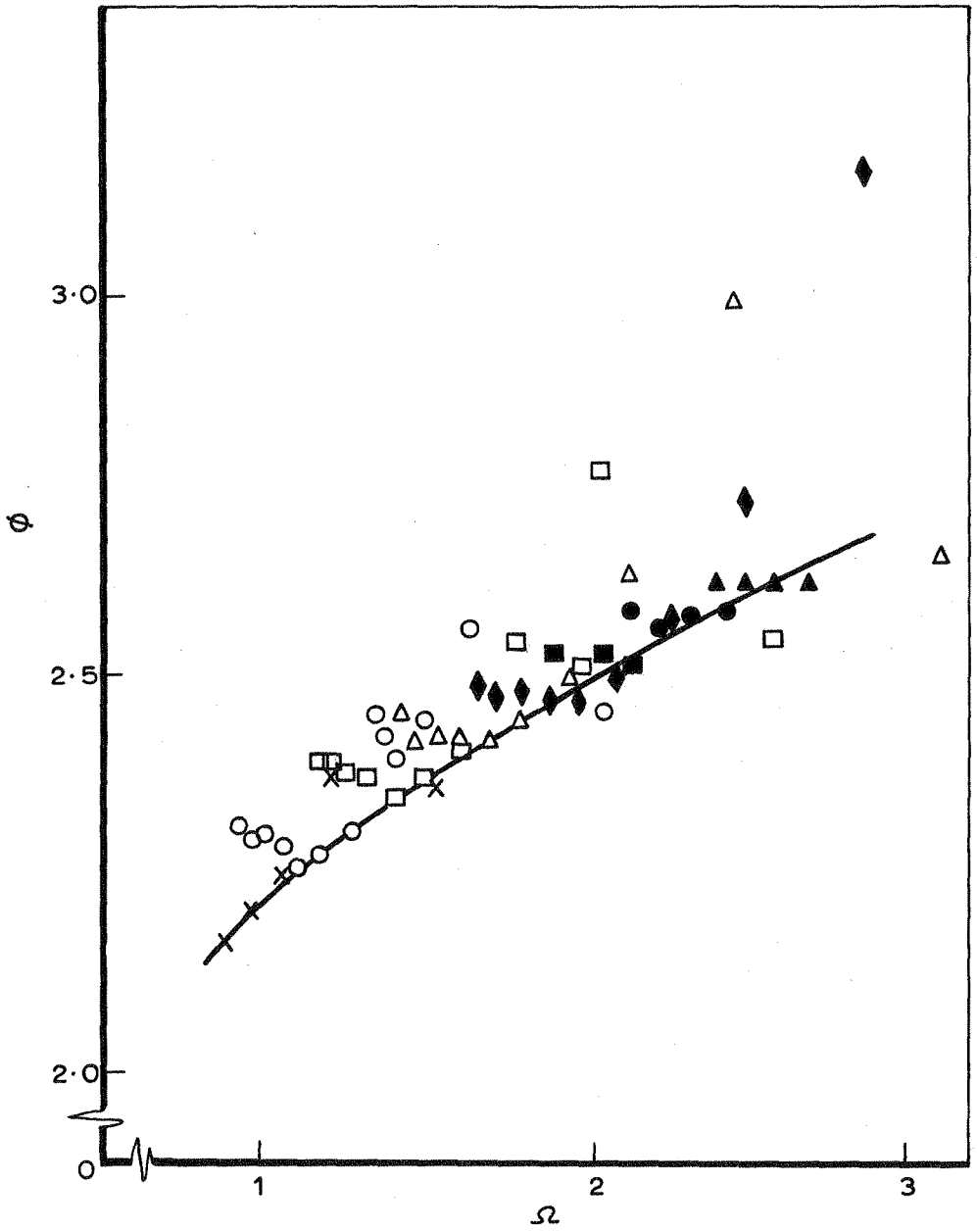

$\frac{z}{x} = 0.0355$ $x = 3ft-9in$ $z = 1{\cdot}6\,in$	
Symbols	Wind speed ft/s
X	1·5
O	2·0
□	2·5
△	3·0
♦	3·5
■	4·0
●	4·5
▲	5·0

1/5108 F.R. 572

FIG. 12. DIMENSIONLESS TEMPERATURE RISES

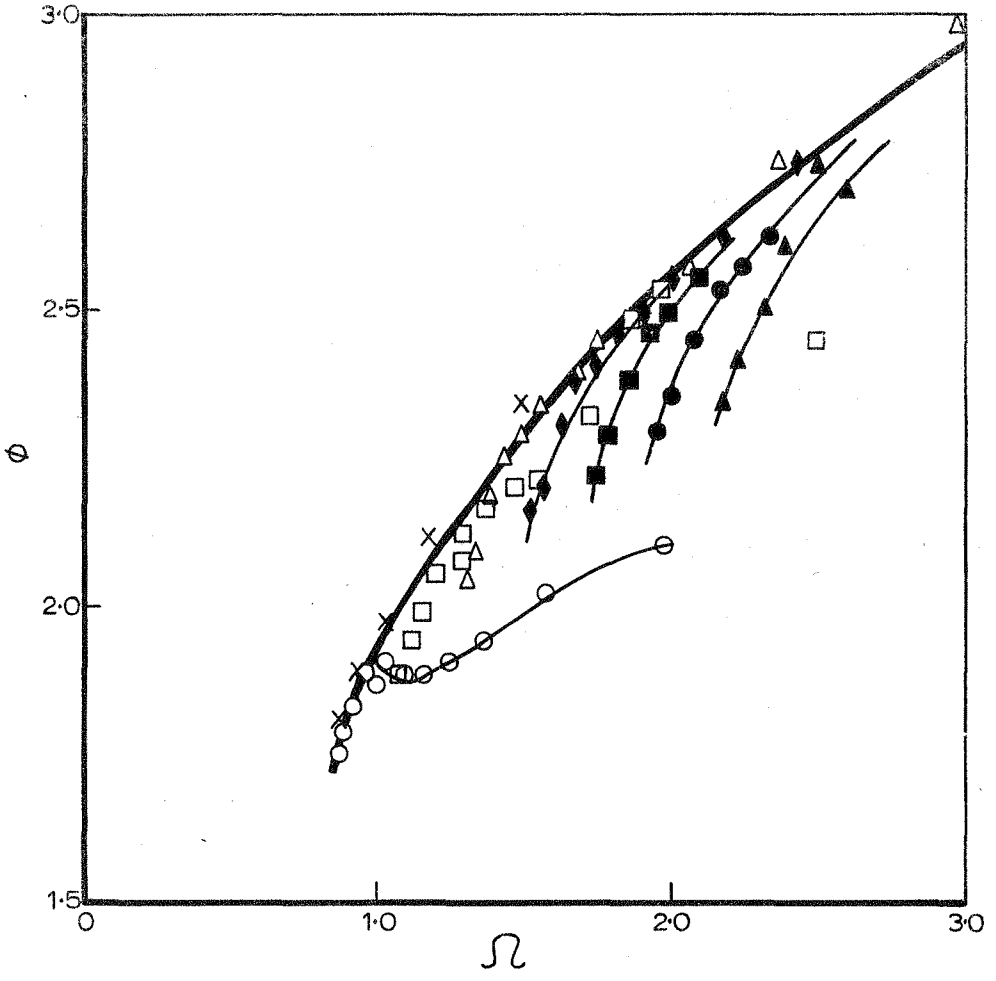

$\frac{z}{x}$ = 0·018 x = 7ft-6in z = 1·6in	
Symbols	Wind speed ft/s
X	1·5
O	2·0
□	2·5
△	3·0
♦	3·5
■	4·0
●	4·5
▲	5·0

1/5109 F.R. 572

FIG. 13. DIMENSIONLESS TEMPERATURE RISES

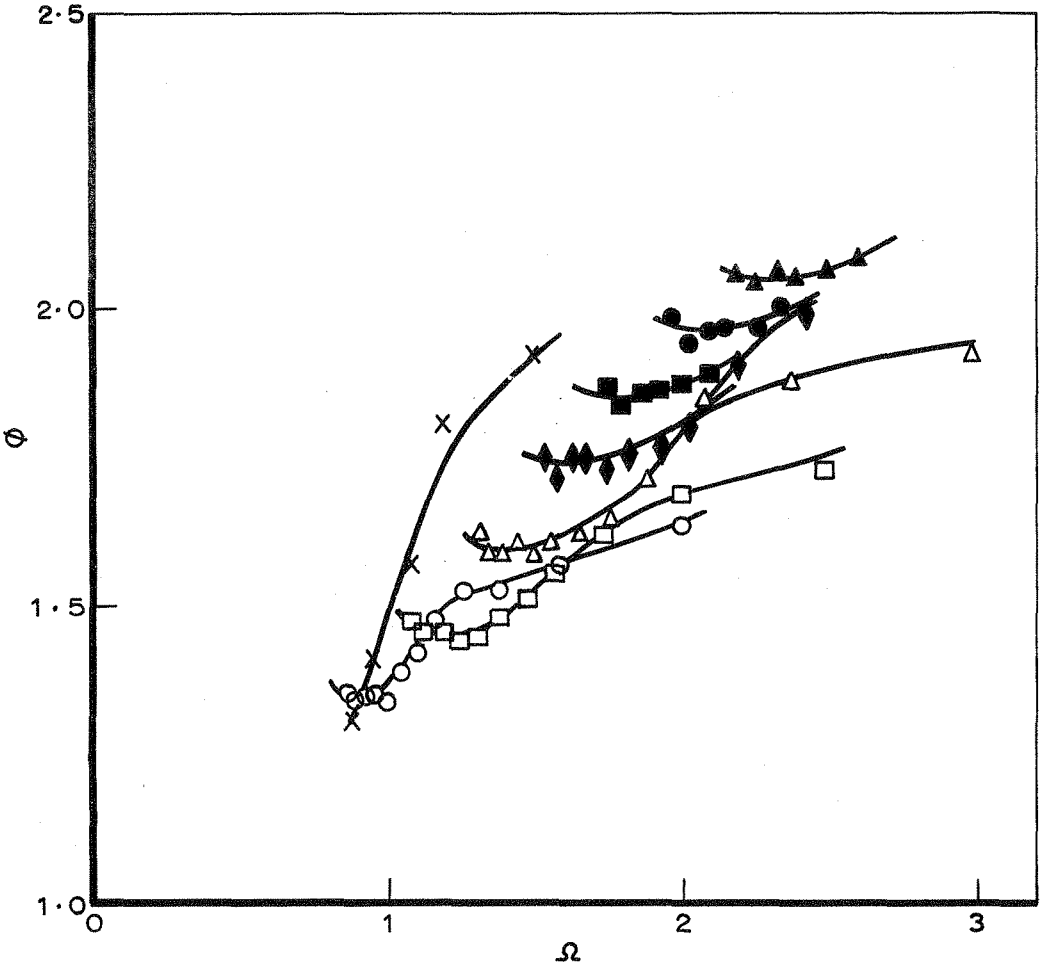

$\frac{z}{x} = 0.0089$ $x = 15ft\text{-}0in \quad z = 1.6\ in$	
Symbols	Wind speed ft/s
X	1·5
O	2·0
□	2·5
△	3·0
♦	3·5
■	4·0
●	4·5
▲	5·0

FIG. 14. DIMENSIONLESS TEMPERATURE RISES

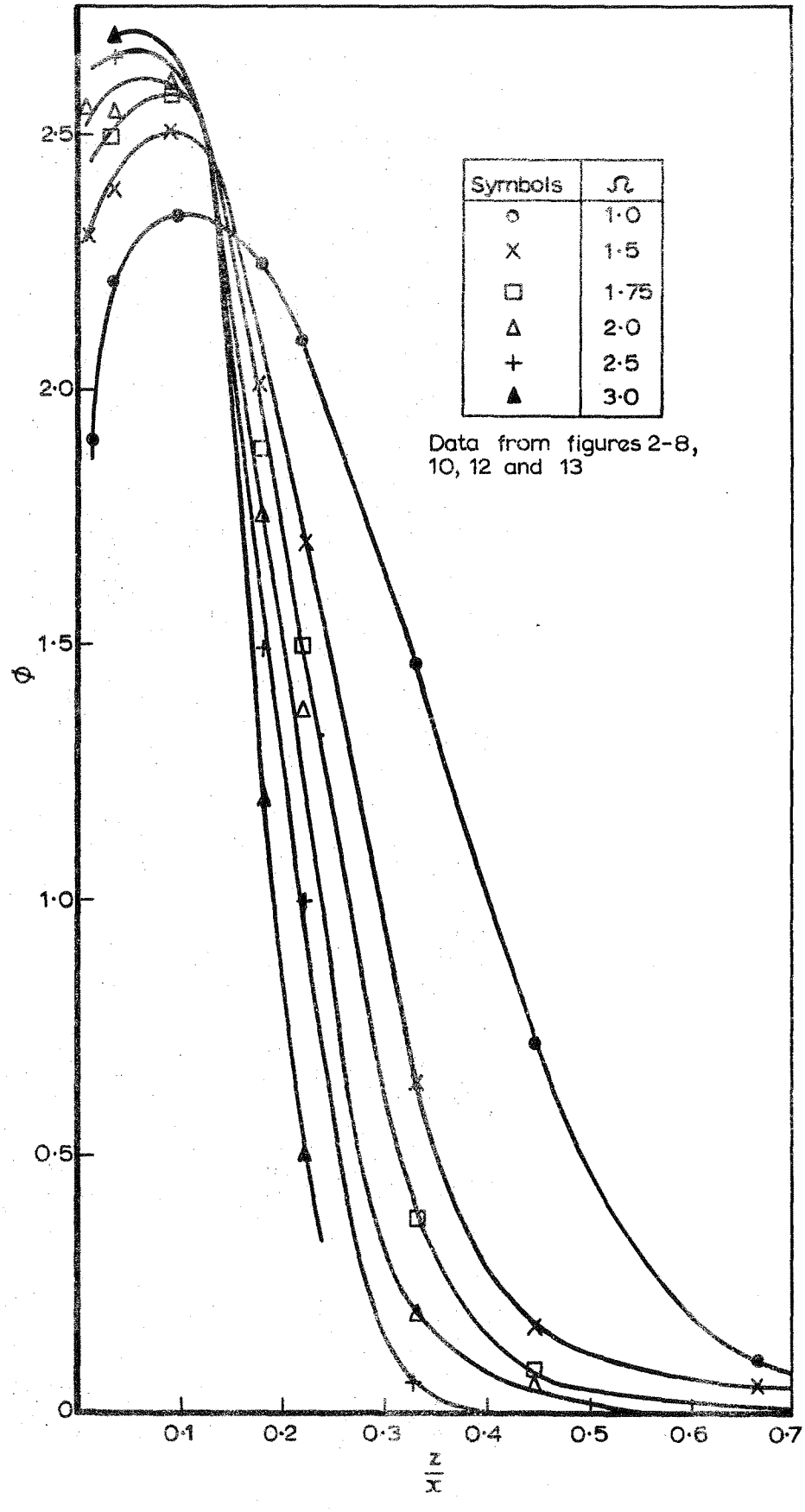

1/5711 F. R. 572

FIG. 15. TEMPERATURE PROFILES

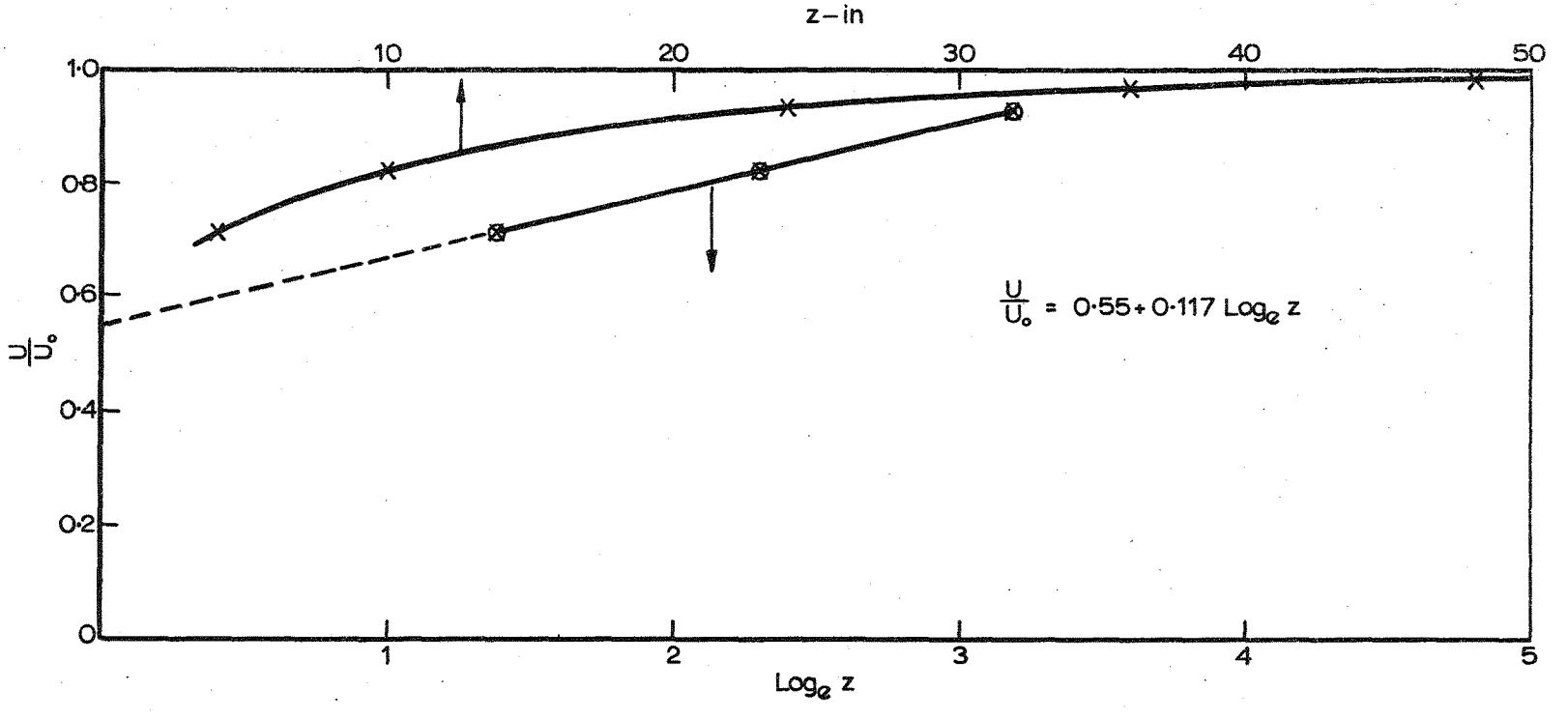

FIG. 16. VELOCITY PROFILE OF UNHEATED AIR

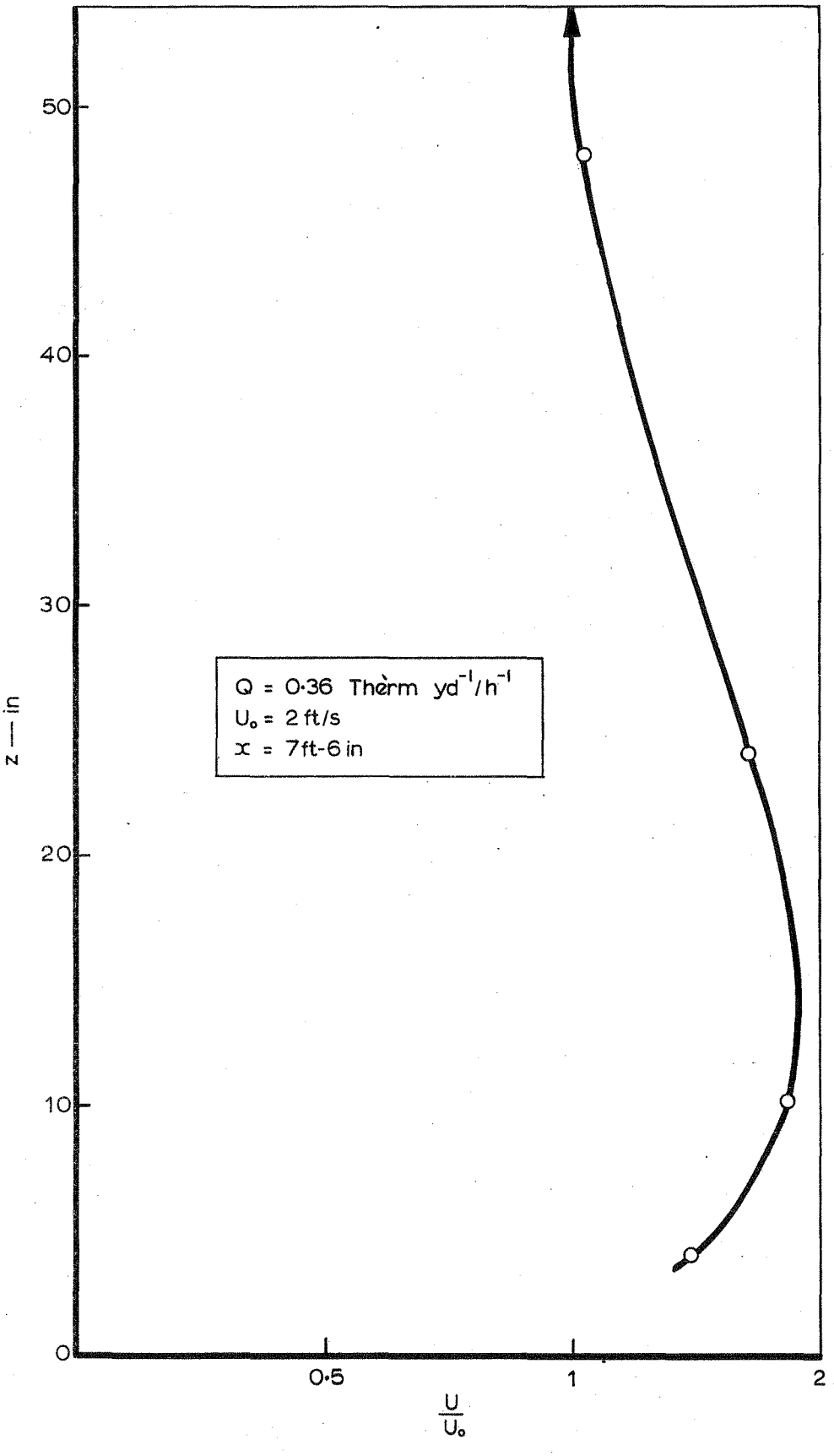

1/5713 F.R. 572

FIG. 17. VELOCITY PROFILE

1/5714 F.R. 572

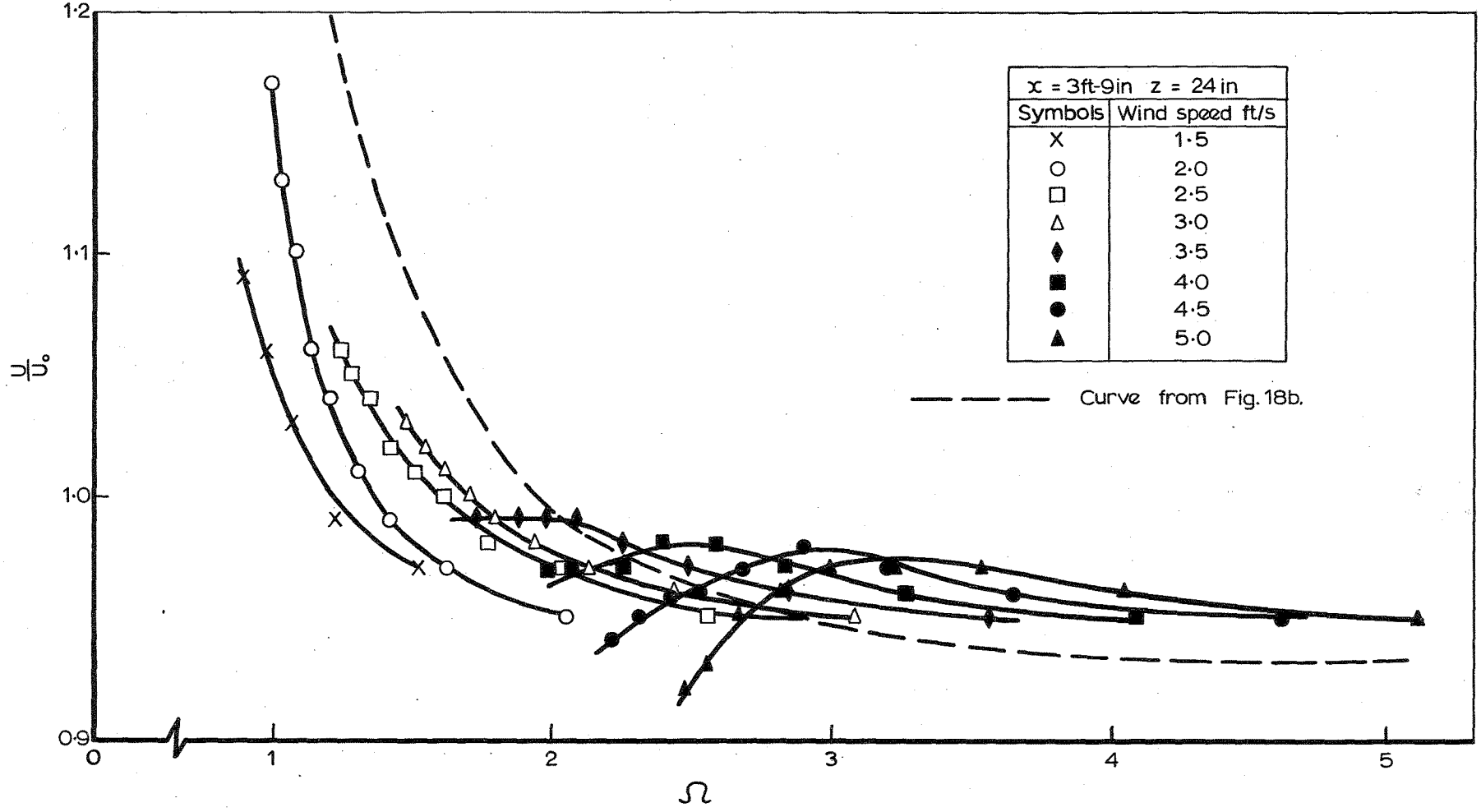

FIG. 18a. LOCAL VELOCITY

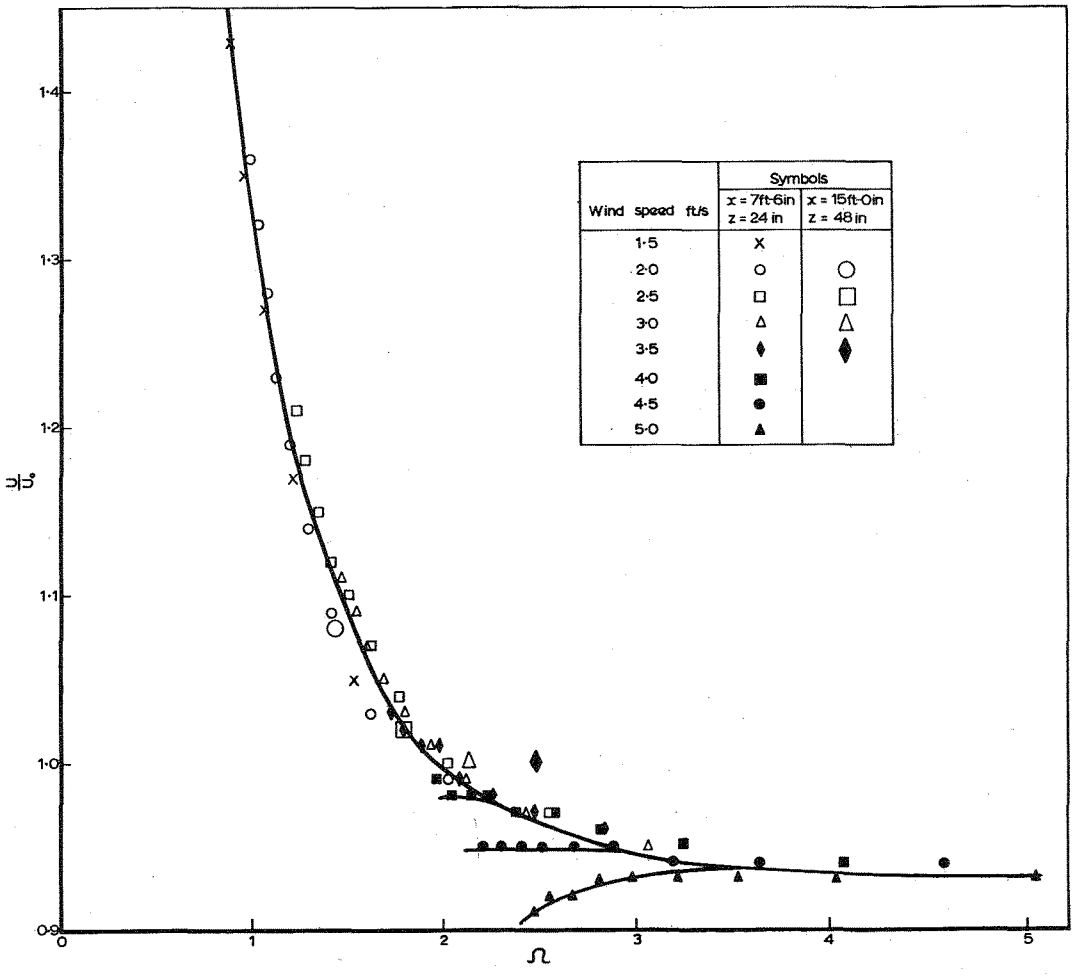

FIG. 18b. LOCAL VELOCITY

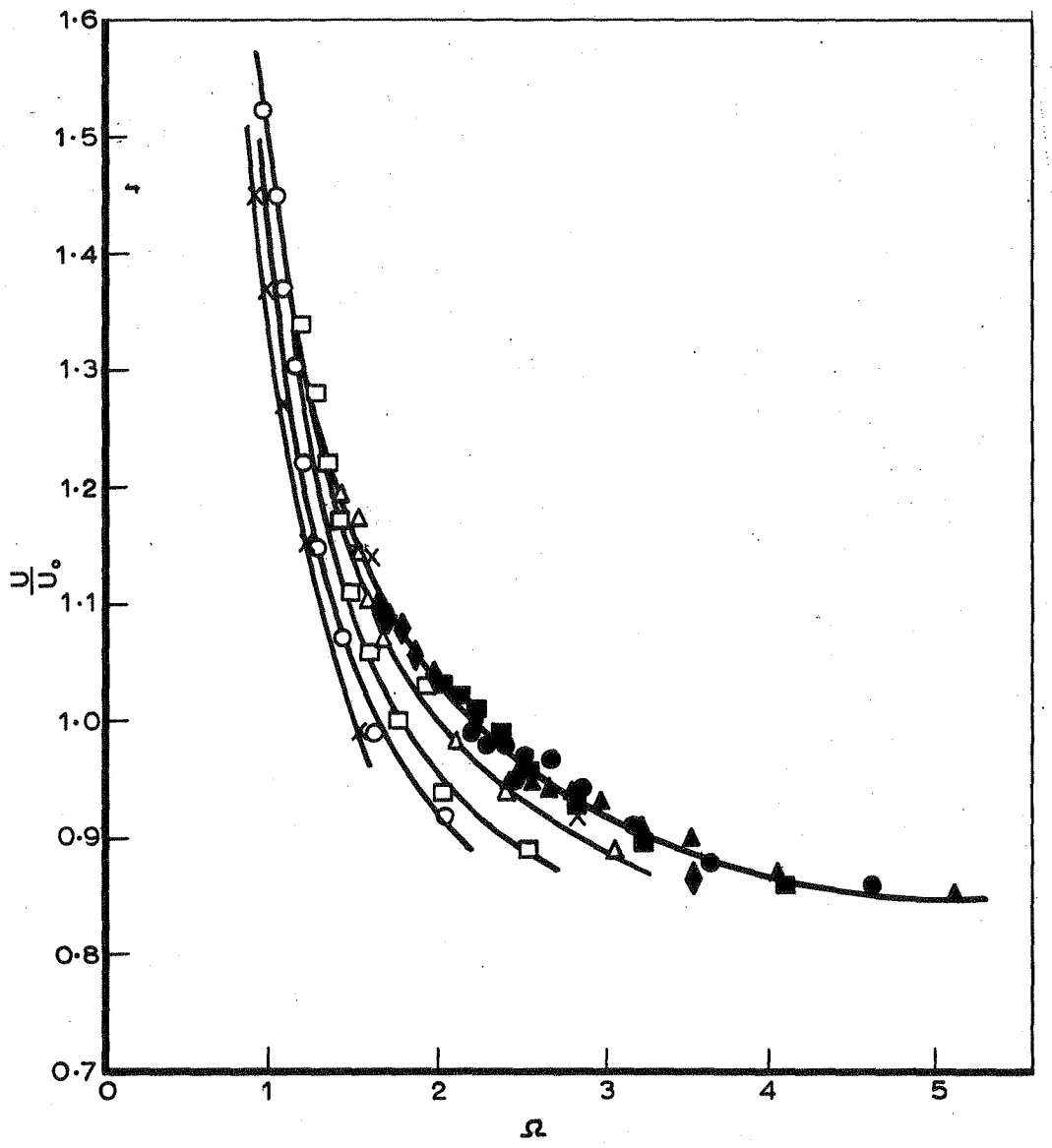

x = 3ft-9in z = 10in	
Symbols	Wind speed ft/s
X	1·5
O	2·0
□	2·5
△	3·0
♦	3·5
■	4·0
●	4·5
▲	5·0

1/5716 F.R. 572

FIG. 19a. LOCAL VELOCITY

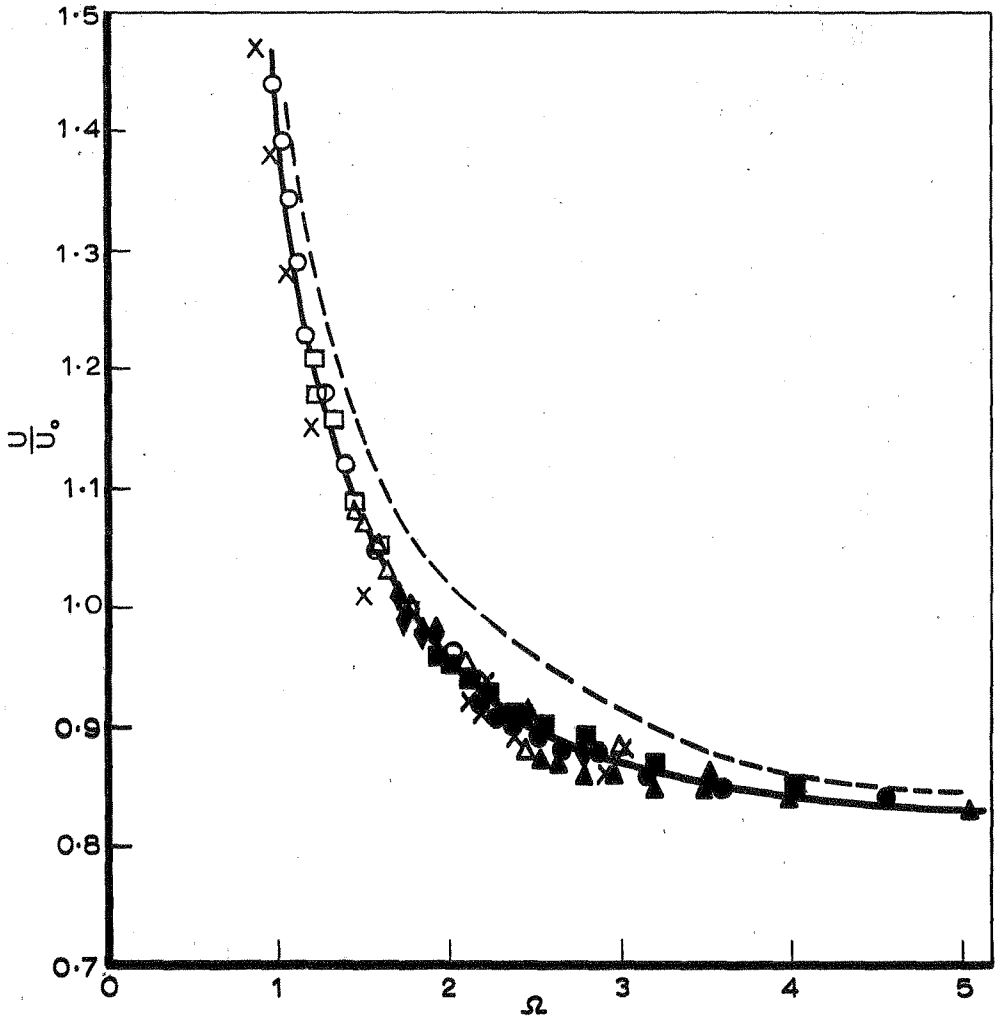

x = 7ft-6in z = 10 in	
Symbols	Wind speed ft/s
×	1·5
○	2·0
□	2·5
△	3·0
♦	3·5
■	4·0
●	4·5
▲	5·0

– – – – Upper curve from Fig. 19a. for x = 3ft-9in z = 10 in

FIG. 19b. LOCAL VELOCITY

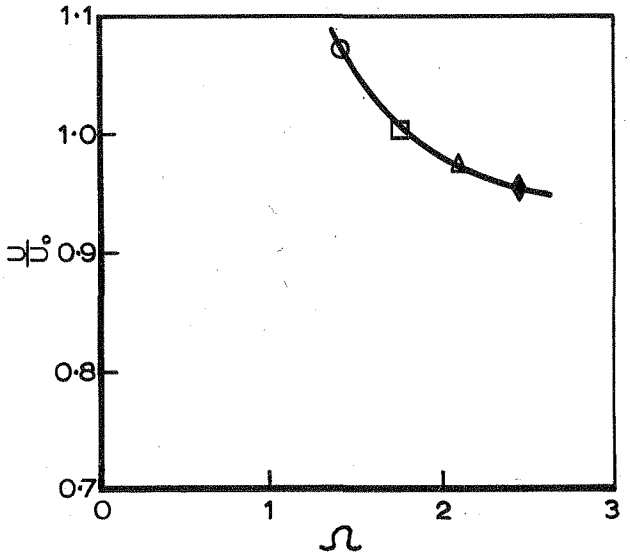

x = 15ft-0in z = 10 in	
Symbols	Wind speed ft/s
○	2·0
□	2·5
△	3·0
♦	3·5

FIG. 19c. LOCAL VELOCITY

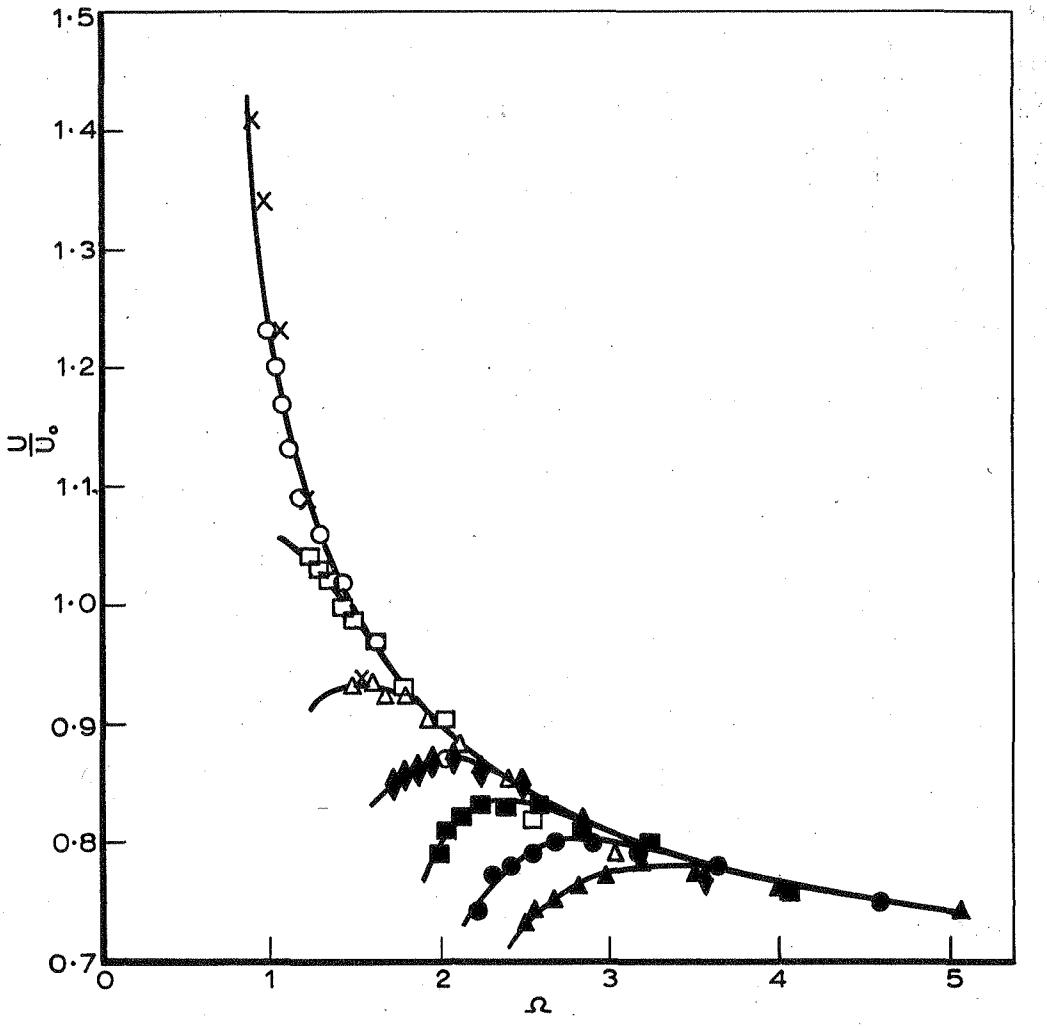

x = 3ft-9in z = 4in	
Symbols	Wind speed ft/s
X	1·5
O	2·0
□	2·5
△	3·0
♦	3·5
■	4·0
●	4·5
▲	5·0

FIG. 20a. LOCAL VELOCITY

I/5719 F.R. 572

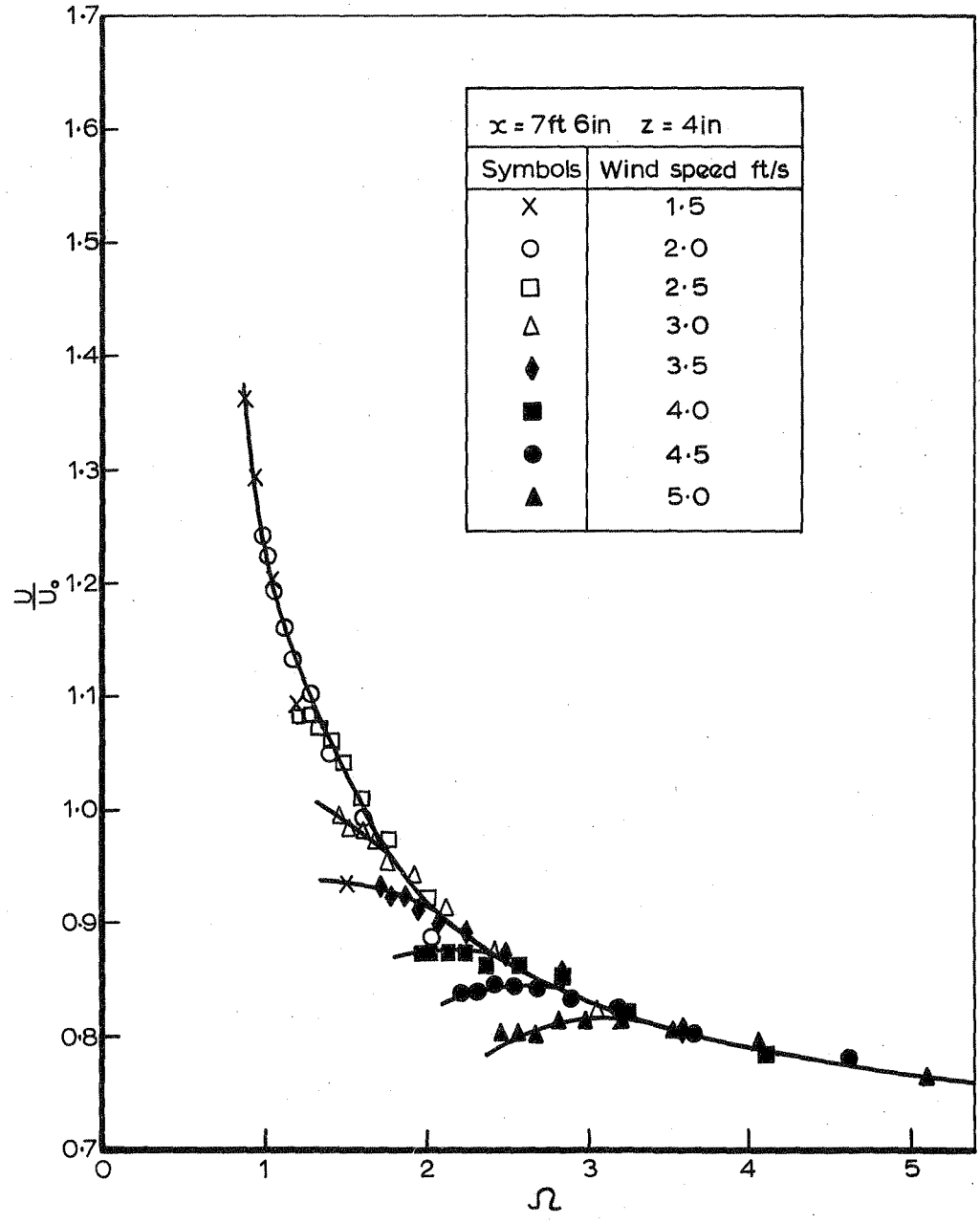

FIG. 20b. LOCAL VELOCITY

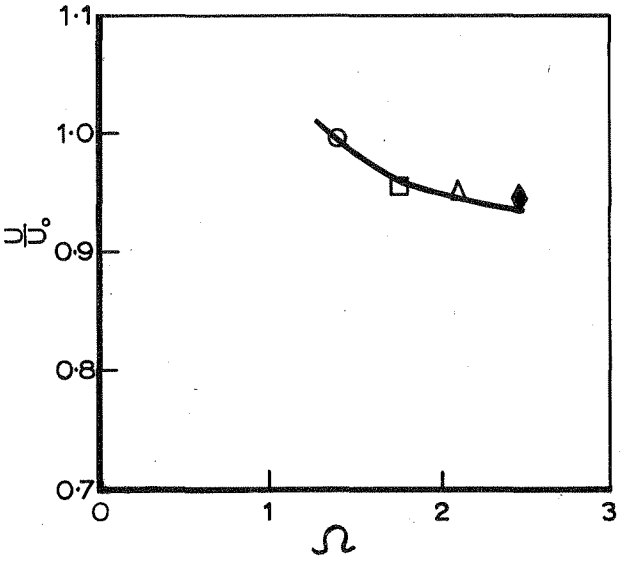

x = 15ft-0in z = 4in	
Symbols	Wind speed ft/s
○	2·0
□	2·5
△	3·0
◆	3·5

FIG. 20c. LOCAL VELOCITY

1/5721 F.R. 572

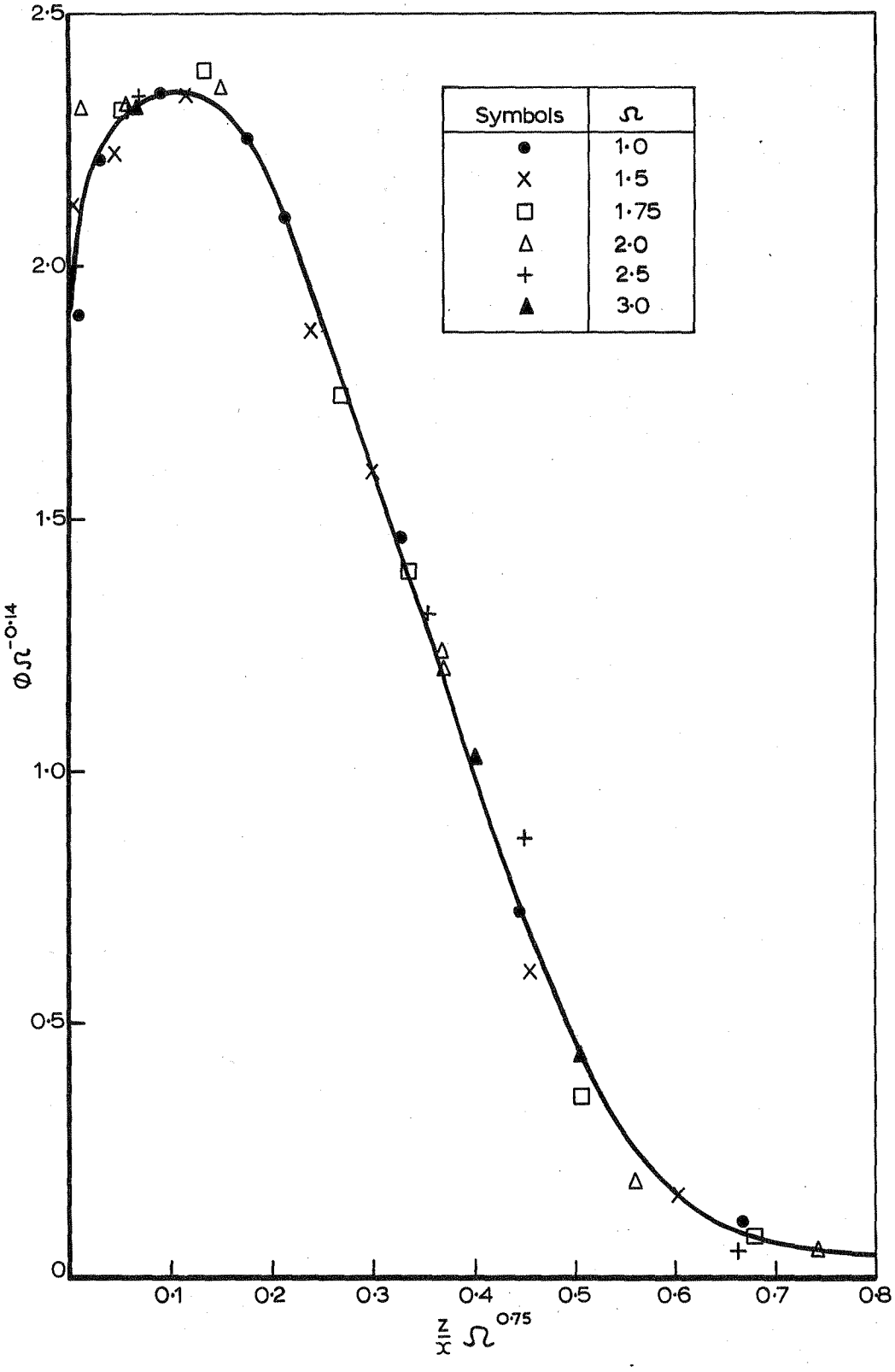

I/5722. F.R. 572

FIG. 21. EMPIRICAL TEMPERATURE PROFILE (BASED ON FIG. 15.)

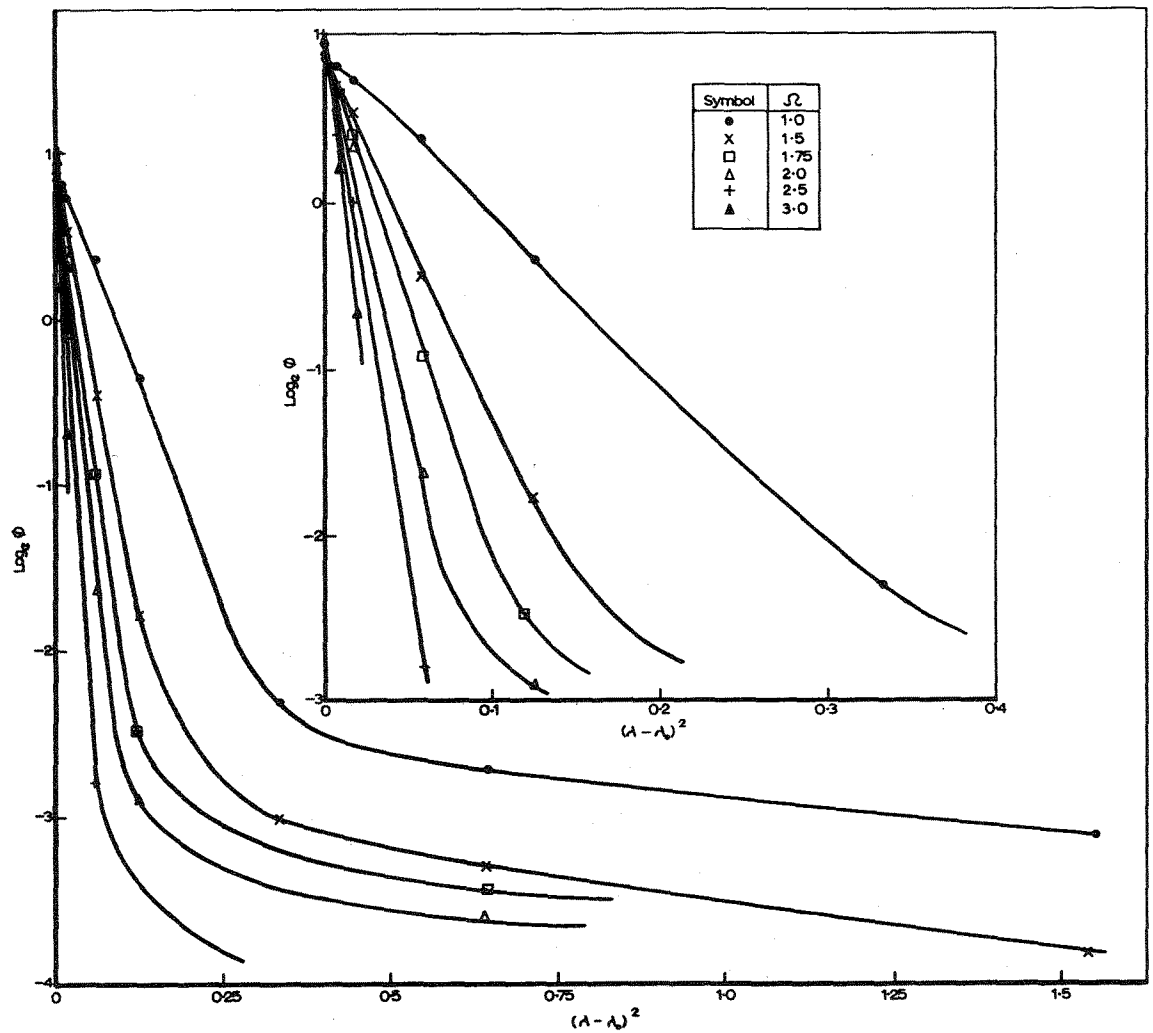

FIG. 22. LOGARITHMIC TEMPERATURE PROFILES

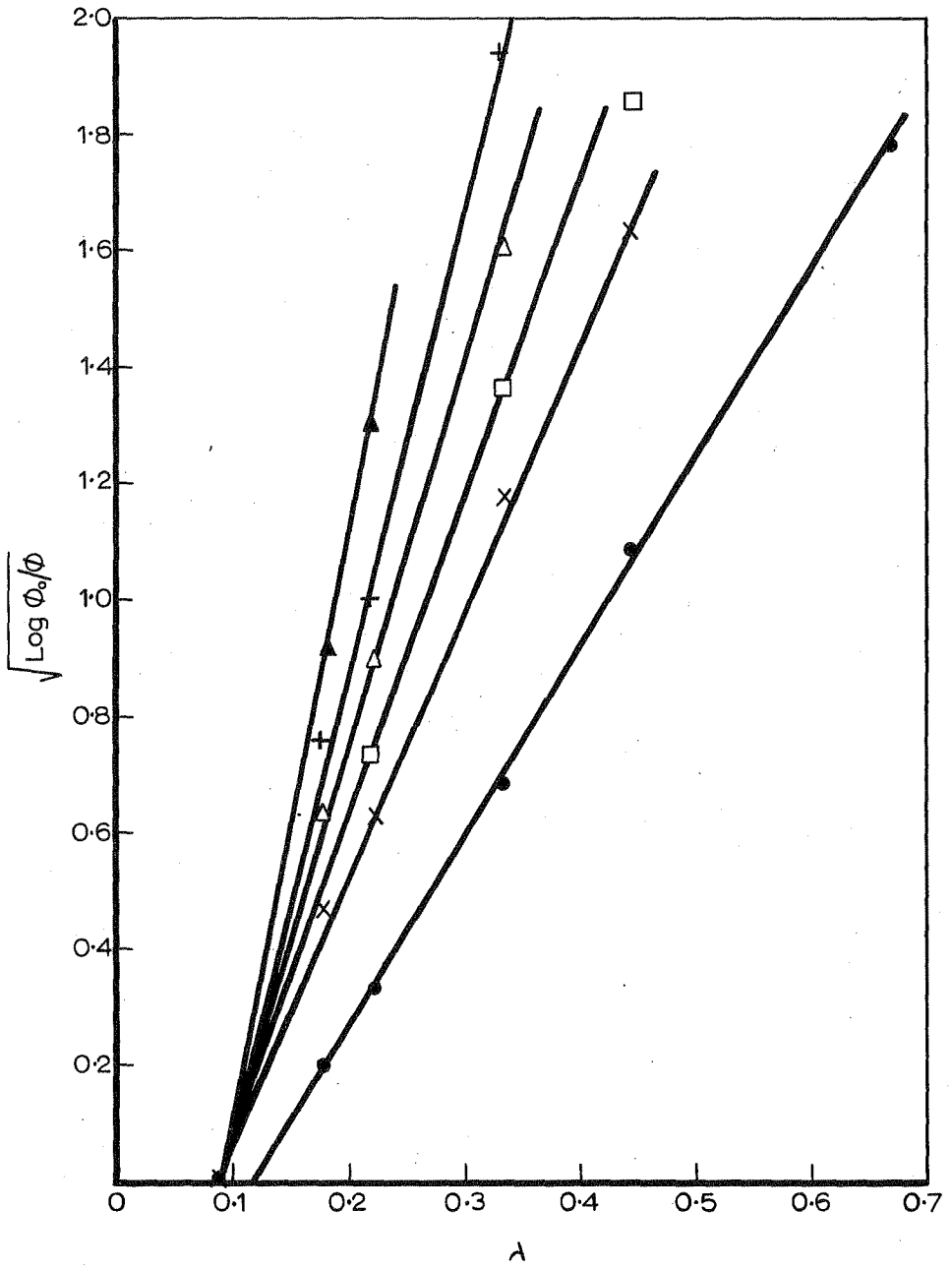

Symbols	Ω
●	1·0
X	1·5
□	1·75
Δ	2·0
+	2·5
▲	3·0

1/5724 F.R. 572

FIG. 23. EVALUATION OF DIFFUSIVITY

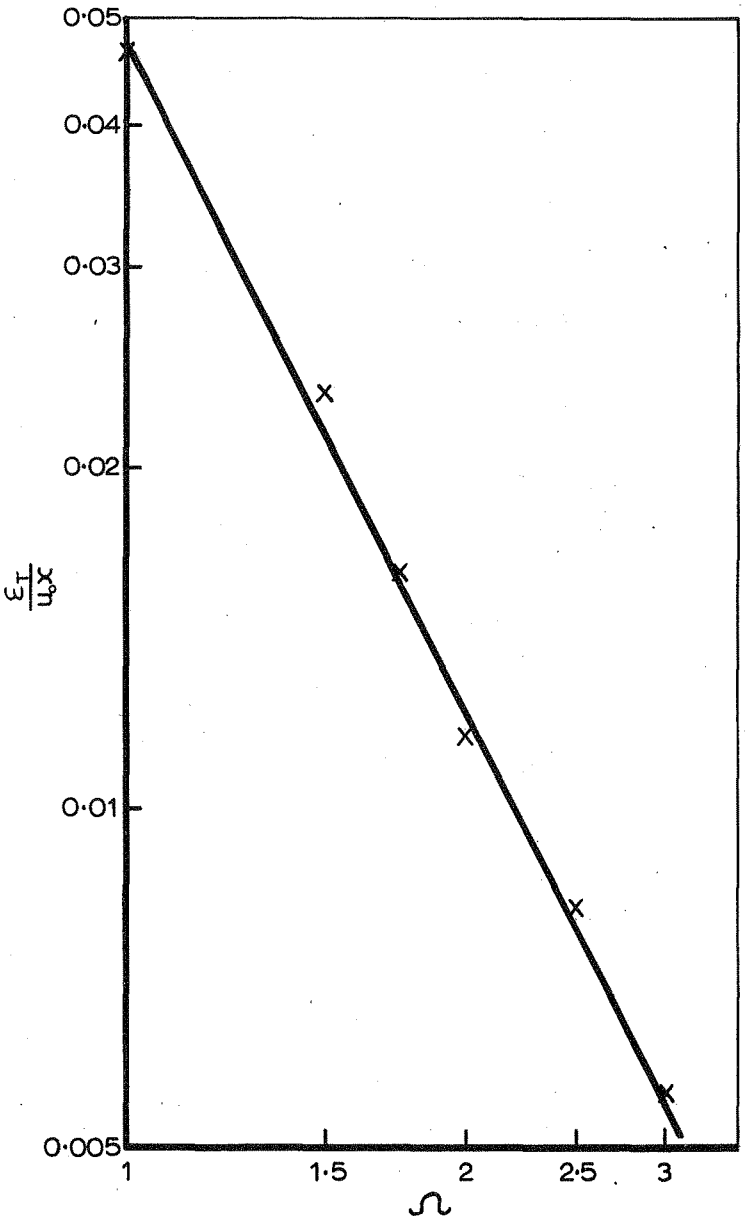

FIG. 24. EFFECTIVE DIFFUSIVITIES

1/5726 F.R. 572